New well-preserved craniodental remains of Simomylodon uccasamamensis (Xenarthra, Mylodontidae) from the Pliocene of the Bolivian Altiplano: phylogenetic, chronostratigraphic, and paleobiogeographic implications

Alberto Boscaini, Timothy J. Gaudin, Bernardino Mamani Quispe, Philippe Münch, Pierre-Olivier Antoine, Francois Pujos

New well-preserved craniodental remains of *Simomylodon uccasamamensis* (Xenarthra: Mylodontidae) from the Pliocene of the Bolivian Altiplano: phylogenetic, chronostratigraphic and palaeobiogeographical implications

AQ1

ALBERTO BOSCAINI[1*], TIMOTHY J. GAUDIN[2], BERNARDINO MAMANI-QUISPE[3], PHILIPPE MÜNCH[4], PIERRE-OLIVIER ANTOINE[5] and FRANÇOIS PUJOS[1]

[1]*Instituto Argentino de Nivología, Glaciología y Ciencias Ambientales (IANIGLA), CCT-CONICET-Mendoza, Avda. Ruiz Leal s/n, Parque Gral. San Martín, 5500 Mendoza, Argentina*
[2]*Department of Biology, Geology, and Environmental Science, University of Tennessee at Chattanooga, 615 McCallie Avenue, Chattanooga, TN 37403-2598, USA*
[3]*Departamento de Palaeontología, Museo Nacional de Historia Natural de Bolivia, Calle 26 s/n, Cota Cota, La Paz, Bolivia*
[4]*Géosciences Montpellier (UMR 5243, CNRS/UM), Université de Montpellier, Montpellier Cedex 05, France*
[5]*Institut des Sciences de l'Evolution de Montpellier, cc64, Université de Montpellier, CNRS, IRD, EPHE, F-34095 Montpellier, France*

Fossil remains of extinct terrestrial sloths have been discovered in numerous localities throughout the Americas, but knowledge of these animals remains poor in the tropical latitudes in comparison with the austral ones. Even where Pliocene mylodontine sloths are known from North and South America, well-preserved craniodental remains are extremely rare, hindering reliable assessment of their taxonomic assignment and phylogenetic affinities. Here, new craniodental remains of *Simomylodon uccasamamensis*, from the latest Miocene–Pliocene of the Bolivian Altiplano, are described and compared with those of other Neogene Mylodontinae from South and North America. The resulting morphological observations, combined with morphometric analyses, permit reliable differentiation among these moderate-sized Miocene–Pliocene mylodontids. *Simomylodon uccasamamensis* appears to be the smallest Pliocene mylodontine, and it is closely related phylogenetically to the late Miocene species *Pleurolestodon acutidens*. *Simomylodon uccasamamensis* is also an endemic taxon of the Andean highlands during the Pliocene, with a continuous chronological range extending throughout the Montehermosan, Chapdamalalan and (early) Marplatan South American Land Mammal Ages. This terrestrial sloth may have found its ideal ecological conditions in the Bolivian Altiplano, during a span of time falling between the important South American Late Miocene–Pliocene faunal turnover and the Great American Biotic Interchange around the Pliocene–Pleistocene transition.

ADDITIONAL KEYWORDS: anatomy – Bolivian Altiplano – 'ground' sloth – Mylodontinae – phylogeny – Pliocene – *Simomylodon uccasamamensis* – Xenarthra.

INTRODUCTION

Extant sloths (Folivora = Tardigrada = Phyllophaga; Delsuc *et al.*, 2001; Fariña & Vizcaíno, 2003) are

*Corresponding author. E-mail: aboscaini@mendoza-conicet.gob.ar, alberto.boscaini@gmail.com

represented by the genera *Bradypus* and *Choloepus*, ecologically and geographically restricted to tropical rain forests of South and Central America. However, the fossil record of sloths extends geographically throughout the Americas and ranges chronologically from the late Eocene to the Holocene (e.g. Gaudin & Croft, 2015). Extinct sloths exhibit much greater

taxonomic diversity and morphological variation than the extant forms, with ≥ 90 recognized genera (e.g. Mones, 1986; McKenna & Bell, 1997) displaying a great variety of dietary habits and locomotor modes (e.g. Bargo *et al.*, 2006; Bargo & Vizcaíno, 2008; Pujos *et al.*, 2012; Toledo, 2016). Their abundance is concentrated especially in Argentina, southern Brazil and the USA, rather than in the tropics. However, this has long been attributed to biases, owing to both the greater accessibility of fossil-bearing deposits (i.e. more open habitats) and the longer palaeontological tradition in the countries that lie outside the tropical latitudes of the American continent (Pujos *et al.*, 2012, 2017; Rincón *et al.*, 2016).

Among Folivora, five monophyletic clades are recognized and traditionally considered as families: Mylodontidae, Megalonychidae, Nothrotheriidae, Megatheriidae and Bradypodidae (e.g. Gaudin, 2004; McDonald & De Iuliis, 2008; Slater *et al.*, 2016). The genus *Pseudoglyptodon* appeared in the late Eocene and is considered the oldest sloth, but its phylogenetic and familial affinities are still unknown; the mylodontids and megalonychids are the first families to radiate in South America, both represented by isolated late Oligocene remains (Pujos & De Iuliis, 2007; McDonald & De Iuliis, 2008; Shockey & Anaya, 2011; Gaudin & Croft, 2015). The mylodontids persisted until the late Pleistocene–earliest Holocene interval, and three subfamilies are recognized by most authors: Mylodontinae, Lestodontinae and Scelidotheriinae (see Pitana *et al.*, 2013 and references therein). Additionally, the subfamilies Octomylodontinae, Nematheriinae and Urumacotheriinae are considered valid by some authors (e.g. Scillato-Yané, 1977; Rinderknecht *et al.*, 2010; Pitana *et al.*, 2013), but their monophyly has never been demonstrated. Consequently, the Scelidotheriinae, Mylodontinae and Lestodontinae remain the only widely accepted mylodontid subfamilies. According to Gaudin (2004), these three clades are monophyletic, but Lestodontinae represents a subgroup of Mylodontinae, thus constituting the tribe Lestodontini. The latter usage is followed here for the clade comprising *Lestodon* and *Thinobadistes*. Following the same author, *Pseudoprepotherium* from the late middle Miocene Colombian locality of La Venta [Laventan SALMA (South American Land Mammal Age); Hirschfeld, 1985; Flynn & Swisher, 1995] is the most basal mylodontine sloth. *Octodontotherium* from the Desedean SALMA of southern Argentina (e.g. Hoffstetter, 1956; Pujos & De Iuliis, 2007) is one step more derived (Gaudin, 2004). The other Mylodontinae included in the comprehensive phylogenetic analysis performed by Gaudin (2004) are *Pleurolestodon* from the late Miocene of Argentina, and the more widespread Pleistocene genera *Mylodon* and *Glossotherium* from South America, and *Paramylodon* from North America (Gaudin, 2004).

The Neogene fossil record of mylodontines is scarce and, even though they range from South to North America, the poor quality of the craniodental remains has often discouraged their inclusion in updated phylogenetic analyses. The Miocene mylodontines that preserve a significant number of craniodental features are *Glossotheriopsis pascuali* Scillato-Yané, 1976, from the Friasian, Colloncuran and Laventan SALMAs of Argentina and Colombia (middle Miocene; Scillato-Yané, 1976; McDonald, 1997) and *Pleurolestodon acutidens* Rovereto, 1914, from the Huayquerian SALMA of Argentina (early Late Miocene; Rovereto, 1914). In his pioneering work, Rovereto (1914) described three *Pleurolestodon* species that were later synonymized by Kraglievich (1921) and Saint-André *et al.* (2010) under the single species *P. acutidens*. The latter authors also established the new species *Pleurolestodon dalenzae* Saint-André *et al.*, 2010, on the basis of a single well-preserved skull discovered in the late Neogene deposits of the Choquecota section (Oruro Department, Bolivia; Saint-André *et al.*, 2010). In this work, the authors also defined the new genus and species *Simomylodon uccasamamensis* Saint-André *et al.*, 2010 from the Pliocene deposits of Ayo Ayo–Viscachani and Pomata-Ayte localities (La Paz and Oruro Departments, respectively, Bolivia; Saint-André *et al.*, 2010). In the Pliocene, *Glossotheridium chapadmalense* (Kraglievich, 1925) is well represented in the Chapadmalalan SALMA of Argentina (Kraglievich, 1925; Cattoi, 1966). Remains tentatively assigned to the latter taxon were also identified in North America (Robertson, 1976) and Bolivia (Anaya & MacFadden, 1995). However, the specimens from North America (including some scanty remains from Mexico) are now assigned to *Paramylodon garbanii* (Montellano-Ballesteros & Carranza-Castañeda, 1986; Morgan, 2008; McDonald & Morgan, 2011).

During the Pliocene, mylodontid terrestrial sloths were widely spread in the Americas. As recent discoveries testify, early members of the clade occupied the central and northern areas of South America in the late Oligocene–early Miocene (Shockey & Anaya, 2011; Rincón *et al.*, 2016). This suggests that attention should be paid to poorly known areas of South America, in order to elucidate the evolutionary history of mylodontid sloths further (Pujos *et al.*, 2012, 2017).

Since the beginning of the 20th century, many palaeontologists have worked in Bolivia, mainly in the Pleistocene deposits of the Tarija Valley (e.g. Ameghino, 1902; Boule & Thévenin, 1920; Hoffstetter, 1963; Takai, 1982; MacFadden *et al.*, 1983, 2013; Takai *et al.*, 1984; Coltorti *et al.*, 2007). More recently, other classic Bolivian localities have been intensively studied, such as the deposits of Tiupampa (e.g. de Muizon, 1991; Gelfo *et al.*, 2009), Quebrada Honda (e.g. Hoffstetter, 1977; Croft, 2007; Pujos *et al.*, 2011) and Salla-Luribay (e.g. Hoffstetter, 1968; Shockey &
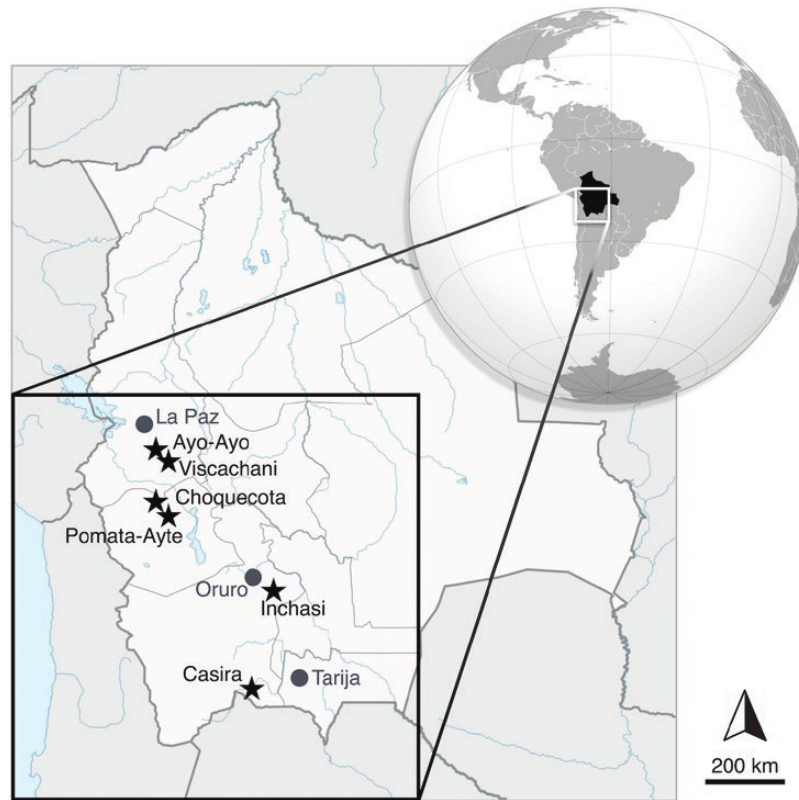
Figure 1. Map of the late Neogene fossil-bearing localities of Bolivia in which the remains of the mylodontid sloth *Simomylodon uccasamamensis* have been recovered.

Anaya, 2008). The area of the Altiplano occupies a large portion of eastern Bolivia, and its fossil richness is still poorly known. This vast region benefited from pioneering work by Robert Hoffstetter (e.g. Hoffstetter 1968, 1977, 1986; Hoffstetter *et al.*, 1971a, b, 1972) and colleagues (e.g. MacFadden *et al.*, 1993; Saint-André, 1994; Anaya & MacFadden, 1995; de Muizon, 1999; Pujos *et al.*, 2016). Pierre-Antoine Saint-André [Institut Français d'Études Andines (IFEA)], together with Federico Anaya [Museo Nacional de Historia Natural, La Paz, Bolivia (MNHN-Bol)], conducted several campaigns in the Bolivian Altiplano in the 1990s, collecting numerous well-preserved fossil vertebrate remains, most of them figured in Saint-André's PhD dissertation (Saint-André, 1994). During the same period, the MNHN-Bol collaborated in excavations with the University of Florida and, since 2005, regular palaeontological campaigns have been conducted in collaboration with Consejo Nacional de Investigaciones Científicas y Tecnicas, Argentina (CONICET). Starting in 2011, the Institut des Sciences de l'Évolution, Montpellier, France (ISEM) has also taken part in the cooperative effort. Some mylodontid remains discovered in these years were published (e.g. Saint-André, 1994; Anaya & MacFadden, 1995;

Saint-André *et al.*, 2010), but many others have long remained undescribed.

The aim of the present work is to present descriptions of many previously unpublished craniodental remains assignable to the extinct sloth *S. uccasamamensis*, providing new data on its morphological variability and new insights on the anatomy, phylogeny and palaeobiogeography of this Andean mylodontid species.

GEOGRAPHICAL   AND   GEOLOGICAL   SETTINGS

The fossil remains assigned to *S. uccasamamensis* and considered in this work (for further details, see Supporting Information, Appendix S1) come from five distinct localities in three departments of the Bolivian Altiplano (Fig. 1). The stratigraphy of deposits has been constrained by geochronological data obtained from various volcanic tuffs interbedded within the sedimentary series (Evernden *et al.*, 1966, 1977; Lavenu *et al.*, 1989; Marshall *et al.*, 1992; MacFadden *et al.*, 1993; Anaya & MacFadden, 1995). In this work, we refine the age of 'Toba 76' (Saint-André, 1994; Saint-André *et al.*, 2010), which is an index-bed tuff occurring throughout the Neogene series of the central Altiplano and near the Miocene–Pliocene transition (Marshall *et al.*, 1992). It

is thus crucial to know the age of 'Toba 76' precisely. This tuff was previously dated by the K/Ar method (Evernden *et al.*, 1966, 1977; Marshall *et al.*, 1992) and by $^{40}Ar/^{39}Ar$ (Marshall *et al.*, 1992). K/Ar ages are very imprecise and cannot be retained. The best estimate is a $^{40}Ar/^{39}Ar$ mean age on four sanidine single crystals at 5.348 ± 0.005 Myr obtained by Marshall *et al.* (1992). These authors retained an age of 5.4 Myr for 'Toba 76', thus pointing to a latest Miocene age. It must be highlighted that the age of the monitor used for age calculation has been recalibrated many times since the work of Marshall *et al.* (1992) (e.g. Renne *et al.*, 2010) and that their error calculation did not consider the error on the irradiation factor, *J*. We performed $^{40}Ar/^{39}Ar$ dating on four single crystals of sanidine (detailed methodology in Supporting Information, Appendix S2) from 'Toba 76' sampled in the studied section from the classic palaeontological site of Pomata (Saint-André, 1994). We obtained four concordant ages (5.26 ± 0.02, 5.25 ± 0.02, 5.27 ± 0.03 and 5.27 ± 0.02 Myr), corresponding to 99.67, 100, 90.43 and 100% of ^{39}Ar released, respectively. We retained the weighted mean age of 5.26 ± 0.02 Myr for 'Toba 76' that points to earliest Pliocene (detailed results in Supporting Information, Appendix S3).

Choquecota

The most important fossil locality lies near the village of Choquecota (Choquecota-Hakallinca; Saint-André, 1994). The classic site is middle Miocene in age (Colloncuran SALMA; Saint-André, 1994) and located 3 km north of the homonym village (Carangas Province, Oruro Department). However, the only specimen of *S. uccasamamensis* from this area was recovered ~3.5 km southwest of Choquecota village, at the top of a Miocene sedimentary sequence capped by the tuff commonly called 'Toba 76' (Saint-André, 1994; Saint-André *et al.*, 2010; see previous subsection). The material of *S. uccasamamensis* was found 15 m below 'Toba 76', in a reddish sandstone layer from the Rosa Pata Formation (late Miocene) unconformably overlain by the Umala Formation (Pliocene; Saint-André *et al.*, 2010). This single specimen (MNHN-Bol V 3348) consists of a partial skull lacking its posterior region (Saint-André, 1994; Saint-André *et al.*, 2010).

Originally assigned by Saint-André (1994) to *Glossotheriscum dalenzae* and later published under the genus *Pleurolestodon* by Saint-André *et al.* (2010), this skull is here assigned to *S. uccasamamensis* on the basis of morphological and morphometric data (see Discussion). This specimen is considered to represent the oldest known remains of *S. uccasamamensis*, immediately before the Huayquerian–Montehermosan transition and most probably predating the Miocene–Pliocene transition.

Pomata-Ayte

This locality, early Pliocene in age, is located 2.5 km east-northeast of the homonym village (Carangas Province, Oruro Department; Saint-André, 1994). Lithostratigraphically, it belongs to the Umala Formation, which lies above the Totora and Pomata Formations. Five metres above the base of the section, 'Toba 76' is recovered. The fossil remains from the Pomata-Ayte locality were found above this tuff, in the basal ~60 m deposits of the Pliocene–Pleistocene Umala Formation (Saint-André *et al.*, 2010).

The vertebrate fauna includes the sloths *S. uccasamamensis*, *Aymaratherium jeani* and *Megatherium (Megatherium) altiplanicum*, the litoptern *Macrauchenia* sp., the toxodontid *Posnanskytherium* cf. *viscachanense*, the pampatheriid *Plaina* sp. and two other armoured cingulates of uncertain affinities, a rodent and a giant carnivorous phorusrhacoid bird. The faunal composition is consistent with an earliest Pliocene age (Montehermosan; Hoffstetter *et al.*, 1972; Marshall *et al.*, 1983; Hoffstetter, 1986; Marshall & Sempéré, 1991; Saint-André, 1994; Pujos *et al.*, 2016).

Casira

The locality of Casira (= Kasira; Suárez-Soruco & Díaz-Martínez, 1996) is situated south-west of the Khellu Khakha Loma Mountain (Modesto Omiste Province, Potosí Department) and close to the Bolivian–Argentinian frontier (Anaya *et al.*, 1989). The age of these deposits is not well established (Anaya *et al.*, 1989). Shockey *et al.* (2007) proposed a Pliocene age for these sediments, whereas Cerdeño *et al.* (2012) considered them late Miocene. However, the presence of *Megatherium (M.) altiplanicum* and the low diversity of the mesotheriid taxa (M. Fernández Monescillo, pers. comm.) suggest that an early Pliocene age (i.e. Montehermosan–Chapadmalalan SALMAs) would be more consistent for the Casira fauna.

Inchasi

The Inchasi locality is situated 50 km southeast of the city of Potosí (Province of Linares, Department of Potosí; MacFadden *et al.*, 1993; Anaya & MacFadden, 1995). Its fossiliferous beds have been dated to between 4.0 and 3.3 Myr (late Early Pliocene; MacFadden *et al.*, 1993; Anaya & MacFadden, 1995). The Inchasi locality is Chapadmalalan in age (Cione & Tonni, 1996) and presents the most diversified Pliocene mammalian assemblage of the Bolivian Altiplano (MacFadden *et al.*, 1993; Anaya & MacFadden, 1995).

The mammalian fauna of Inchasi includes the notoungulates *Posnanskytherium* and *Hypsitherium*, two endemic genera of the Bolivian Altiplano, and many other mammals typical of the Pliocene of Argentina, such as *Promacrauchenia*, *Caviodon*, *Chapalmatherium*, *Paraglyptodon*, *Plohophorus* and *Plaina* (MacFadden

et al., 1993; Anaya & MacFadden, 1995). In Inchasi, sloths are represented by some unidentified remains of Mylodontidae and Megatheriidae and by *Proscelidodon patrius* and *Glossotheridium chapadmalense* (Anaya & MacFadden, 1995). The latter species is represented by three mandibles that are here reassigned to *S. uccasamamensis* on the basis of morphological and morphometric data (see Discussion).

Ayo Ayo–Viscachani
The Ayo Ayo–Viscachani locality is situated between the two homonym villages in the Aroma Province (La Paz Department), ~70 km south of the city of La Paz (e.g. Hoffstetter *et al.*, 1971b; Marshall & Sempéré, 1991; Saint-André, 1994). The fossils come from the upper part of the Umala Formation, which ranges the late Pliocene and is further coeval with the Remedios Formation found at more southern latitudes (Lavenu, 1984). The sandy and clayish deposits at Ayo Ayo–Viscachani provide both late Pliocene and Pleistocene vertebrate assemblages (i.e. Hoffstetter *et al.*, 1971b). Pliocene and Pleistocene layers were seemingly deposited conformably (Saint-André, 1994). However, the two successive faunas present distinct faunal associations and are separated by volcanic ashes (the Ayo Ayo tuff), which yield a mean age of ~2.8 Myr (Lavenu *et al.*, 1989; Marshall *et al.*, 1992; Saint-André, 1994).

The Pliocene fauna includes the marsupials *Sparassocynus heterotopicus* and *Microtragulus bolivianus*, the litoptern *Macrauchenia minor* and the notoungulate *Posnanskytherium* cf. *P. viscachanense*, the rodents *Praectenomys*, *Praectenomys*, cf. *Lagostomopsis* and *Chapalmatherium*, and the armoured xenarthrans *Pampatherium* sp. and *Macroeuphractus* cf. *moreni* (Saint-André, 1994 and references therein). Sloths are assigned to the giant megatheriid *Megatherium* (*M.*) *altiplanicum* and the mylodontid *S. uccasamamensis* (Saint-André, 1994; Saint-André *et al.*, 2010).

According to the latest proposed adjustments of the biochronological and geochronological scales (Reguero *et al.*, 2007; Tomassini *et al.*, 2013), the late Pliocene period roughly coincides with the early Marplatan SALMA (Barrancolabian and Vorohuean subages).

Overall, the remains of *S. uccasamamensis* are from deposits that are virtually bracketed below by 'Toba 76', which we consider now dated at 5.26 ± 0.02 Myr, and above by the 2.8 Myr Ayo Ayo tuff, which correspond to the base and the top of the Umala Formation and roughly coincide with the Pliocene (Marshall & Sempéré, 1991).

MATERIAL AND METHODS

r emains   examined   and   comparative   sample

The new craniodental remains of *S. uccasamamensis* (Supporting Information, Appendix S1) are housed in the MNHN-Bol of La Paz (Bolivia). They consist of several well-preserved skulls and mandibles that, in addition to the remains previously presented by Saint-André *et al.* (2010), extend our knowledge of the morphology and the intraspecific variation of this poorly known mylodontid extinct sloth.

The observed features are compared with the other well-known mylodontids, especially the Neogene taxa from both South and North America housed in the following institutions: AMNH, American Museum of Natural History, New York, NY, USA; FMNH, Field Museum of Natural History, Chicago, IL, USA; MACN, Museo Argentino de Ciencias Naturales 'Bernardino Rivadavia', Buenos Aires, Argentina; MLP, Museo de La Plata, La Plata, Argentina; MMP, Museo Municipal de Ciencias Naturales 'Lorenzo Scaglia', Mar del Plata, Argentina; MNHN-Bol, Museo Nacional de Historia Natural de Bolivia, La Paz, Bolivia; MNHN.F, fossil collection of the Muséum national d'Histoire naturelle, Paris, France; and UF, University of Florida, Florida Museum of Natural History (FLMNH), Gainesville, FL, USA.

Descriptions, comparisons and measurements were conducted by first-hand examination of the specimens, with the exception of the holotype of *Pleurolestodon acutidens* MACN Pv 2952–2953. This specimen is missing from the vertebrate palaeontological collection of MACN (Curator A. Kramarz, pers. comm.). However, the morphological and morphometric comparisons have been conducted on the basis of the photographs and measurements made available by Rovereto (1914). The set of measurements performed on the skull, mandibles and both upper and lower dentition of mylodontid taxa is based, with some modifications, on the unpublished PhD dissertation of Esteban (1996) (Supporting Information, Appendix S4). Measurements were taken with a digital calliper to the nearest 0.1 mm (Supporting Information, Appendix S5).

s tatistical   and   phyloGenetic   analyses

The principal components analyses (PCAs) were conducted on the set of craniodental measurements (Supporting Information, Appendices S4 and S5) using the program PAST v.3.11 (Hammer *et al.*, 2001). Owing to the paucity of crania associated with mandibles, these two anatomical regions (i.e. crania and mandibles, with their respective dentitions) were considered separately in the multivariate analyses. The PCAs were conducted on a reduced subset of specimens and variables, in order to minimize the data missing because of preservation (for further details, see Supporting Information, Appendix 5). In this way, the missing data imputation, conducted using the 'mean

value imputation' algorithm (the default option of PAST v.3.11), was reduced to a minimum. Percentages of explained variance and the main loadings of the single variables are reported in the Supporting Information (Appendix S6).

The data matrix for our phylogenetic analysis is that of Gaudin (2004), including 46 taxa and 286 osteological characters. The species *S. uccasamamensis* was added to this matrix using the program Mesquite (Maddison & Maddison, 2011). The phylogenetic analysis was performed using the parsimony software TNT v.1.5 (Goloboff *et al.*, 2008), under the 'traditional search' algorithm. We used as outgroups four extant representatives of Cingulata and Vermilingua from the study by Gaudin (2004) (i.e. *Euphractus*, *Cyclopes*, *Myrmecophaga* and *Tamandua*). All the other outgroup taxa present in Gaudin's work were inactivated using the 'inactive taxa' function available in TNT. In this way, it was possible to run the analysis without applying the a priori constraint to the structure of the outgroup taxa used by Gaudin (2004). Moreover, all the non-mylodontid sloths were inactivated a priori, with the exception of the modern three-toed sloth *Bradypus* and the Santacrucian megatherioid *Hapalops*, which were also used as outgroups.

The analysis was conducted following the procedure of Gaudin (2004), using equally weighted characters and maintaining the same ordination of the characters; namely, of the 286 osteological characters, 129 were multistate and of these, 50 were unordered (for further details, see Gaudin, 2004). Support values were calculated using total Bremer support (Bremer, 1994), bootstrap (Felsenstein, 1985) and jackknife (Farris *et al.*, 1996) resampling methods. The codification of *S. uccasamamensis*, together with the support values at each node, are available in the Supporting Information (Appendix S7).

The result, a single most parsimonious tree (MPT; see Results subsection 'Phylogenetic analysis') was then imported into the software environment R (R Development Core Team, 2013) for the temporal calibration. The calibration of the MPT was obtained using the temporal ranges of fossil taxa taken from the literature (Supporting Information, Appendix S8). The time-scaled tree was obtained with the timePaleoPhy function of the package 'paleotree' (Bapst, 2012), setting a minimal branch length of 0.5 Myr. Finally, the time-scaled phylogeny was plotted against the international geological time scale using the function geoscalePhylo of the package 'strap' (Bell & Lloyd, 2015). The script was modified by introducing the absolute chronology of the SALMAs, according to the latest calibrations provided by Slater *et al.* (2016) (Supporting Information, Appendix S9).

a bbreviations

Anatomical abbreviations

Cf, upper caniniform tooth; cf, lower caniniform tooth; Mf, upper molariform tooth; mf, lower molariform tooth.

Other abbreviations

GB, GEOBOL, (former) Servicio Geológico de Bolivia, La Paz, Bolivia; NALMA, North American Land Mammal Age; SALMA, South American Land Mammal Age.

RESULTS

SYSTEMATIC PALAEONTOLOGY

s uperorder   x enarthra   c ope , 1889

o rder   p ilosa   F lower , 1883

s uborder   F olivora   d elsuc *et al* ., 2001

F amily   m ylodontidae   G ill , 1872

s ubFamily   m ylodontinae   G ill , 1872

Genus   *Simomylodon*   s aint -a ndré *et al* ., 2010

Simomylodon   *uccaSamamenSiS*   s aint -a ndré *et al* ., 2010

(F iGs 2–12; s upportinG i nFormation , a ppendix s1)

Glossotheriscum dalenzae Saint-André, 1994: 174–183, fig. 18, pl. 13.

Simotherium uccasamamense Saint-André, 1994: 184–228, figs 19–20, pls 14–20.

Glossotheridium chapadmalense Anaya & MacFadden, 1995: 94–98, figs 3–5, table 1.

*Pleurolestodon dalenzae* Saint-André *et al.*, 2010: 261–269, figs 2–4, table 1.

Nomenclatural observations

The species *Pleurolestodon dalenzae* was erected by Saint-André *et al.* (2010) only a few pages before *S. uccasamamensis*. However, the 'page priority criterion' has no formal standing in the International Code of Zoological Nomenclature (ICZN), and these species have to be considered equally old (see ICZN, 1999). In these cases, the order of priority is determined by the first reviser [i.e. the first author(s) to consider their synonymy; ICZN, 1999, article 24.2]. As first revisers, we therefore establish that *Pleurolestodon dalenzae* is a junior synonym of *S. uccasamamensis*, on the basis of the more abundant and well-determined material of the latter species in comparison with the former (Saint-André *et al.*, 2010).

Holotype

MNHN-Bol V 11731 (ex GB 078; Fig. 2), anterior part of cranium without dentition (Saint-André *et al.*, 2010).
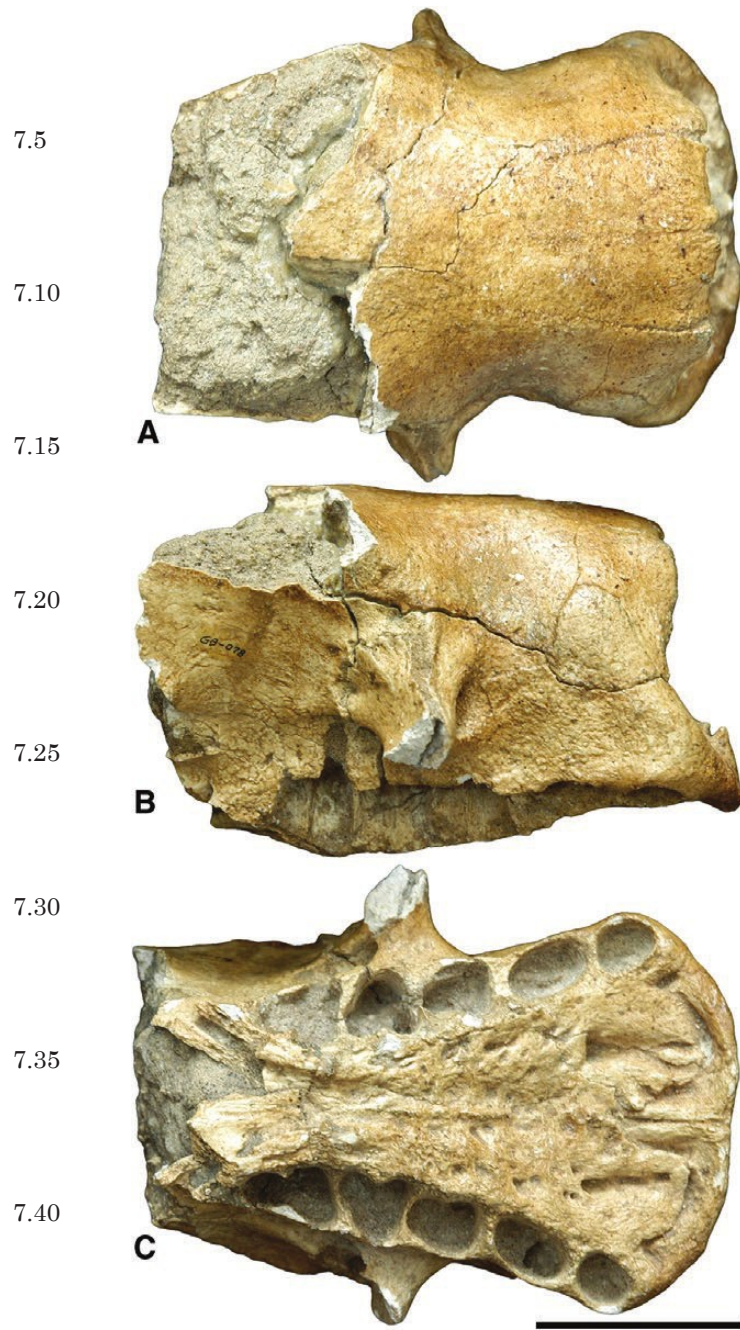
Figure 2. Anterior portion of the cranium of *Simomylodon uccasamamensis* (holotype, MNHN-Bol V 11731; ex GB 078) in dorsal (A), lateral (B) and ventral (C) views. Scale bar: 5 cm.

Paratype
MNHN-Bol V 3321 (Fig. 3), maxillary and premaxillary fragments with left Mf1–Mf3 and right Mf2–Mf4 (Saint-André *et al.*, 2010).

Referred specimens
See the Supporting Information (Appendix S1).

Measurements
See the Supporting Information (Appendix S5).

Revised stratigraphic and geographical occurrence
Latest Miocene–earliest Pliocene of Choquecota, early Pliocene of Pomata-Ayte, Casira and Inchasi (Oruro and Potosí Departments, Bolivia) and late Pliocene of Ayo Ayo–Viscachani (La Paz Department, Bolivia).

Revised diagnosis
Fossil sloth smaller in size than *Glossotheridium chapadmalense*, *Paramylodon garbanii* and *Pleurolestodon acutidens*, and roughly biometrically similar to *Glossotheriopsis pascuali*; long zygomatic processes of squamosal; wide braincase in relationship to the total cranial length and wide V-shaped palate; in ventral view, the medial palatal process of the maxilla is more extended mediolaterally than anteroposteriorly and the occipital condyles are well separated from the condyloid foramina, as in the Miocene species *Pleurolestodon acutidens*; the foramen magnum shows a detached notch located on its dorsal border, similar to that observed in *Pleurolestodon* and *Mylodon*; long and slender ascending process of the jugal, which strongly resembles that of *Glossotheridium chapadmalense*; the diastema between Cf1 and Mf1 is absent or extremely reduced and, in lateral view, Cf1 presents an almost vertical wear facet similar to the condition in *Pleurolestodon acutidens*; Mf2 and Mf3 possess a marked lingual sulcus, comparable to *Pleurolestodon acutidens* and *Paramylodon garbanii*; cf1 is bevelled, with well-developed mesial and distal wear surfaces; mf3 is marked by a deep apicobasal sulcus on its lingual side, absent on the labial side and not covered by the ascending ramus of the mandible in lateral view (like *Glossotheridium chapadmalense* and unlike *Pleurolestodon acutidens* and *Paramylodon garbanii*); the symphyseal spout is anteriorly flat as in *Glossotheridium chapadmalense* and not rounded as in *Pleurolestodon acutidens* and *Paramylodon garbanii*.

Description
Cranium: The cranium of *S. uccasamamensis* appears elongated, with the cranial roof and cranial base roughly horizontal in lateral view. The nasal region is slightly depressed in relationship to the braincase. In dorsal view, MNHN-Bol V 3348 (Fig. 4A), 3711 (Fig. 5A) and 3726 (Fig. 6A) are more slender than MNHN-Bol V 3717 (Fig. 7A) and 3718 (Fig. 8A) (see measurements in Supporting Information, Appendix S5). The snout is elevated and widened anteriorly and relatively short; the braincase is wide in relationship to the total cranial length (Figs 5A, 7A, 8A).

In dorsal view, the nasals are narrow at the level of the antorbital constriction, and gradually broaden anteriorly and posteriorly (Figs 2A, 4A, 5A, 6A, 7A,
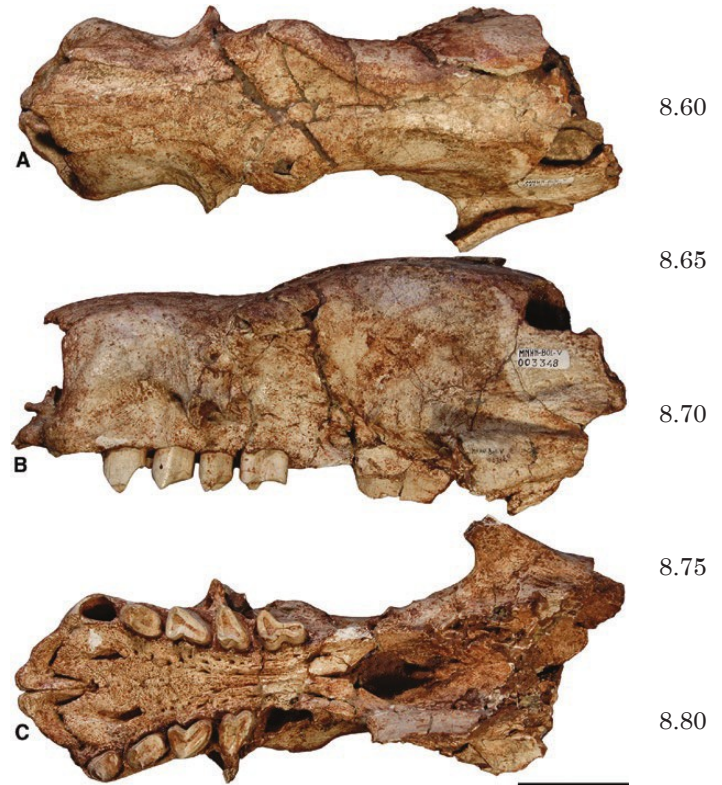
8.5

8.10

8.15

8.20

8.25

8.30

Figure 3. Maxillary and premaxillary fragments of *Simomylodon uccasamamensis* (paratype, MNHN-Bol V 3321) in lateral (A) and ventral (B) views. Scale bar: 5 cm.

8.60

8.65

8.70

8.75

8.80

8.85

Figure 4. Cranium of *Simomylodon uccasamamensis* (MNHN-Bol V 3348) in dorsal (A), lateral (B) and ventral (C) views. Scale bar: 5 cm.

8.35

8.40

8.45

8.50

8.55
8.56

8A). The nasals are probably wider in MNHN-Bol V 3718 (Fig. 8A) than in the other specimens as a result of diagenetic dorsoventral compression of this skull. A V-shaped, posteriorly pointed nasofrontal suture is present in all specimens examined. The anterior border of the nasals is strongly convex in MNHN-Bol V 3711 and 3726 (Figs 5A, 6A) and straighter in MNHN-Bol V 11731, 3717 and 3718 (Figs 2A, 7A, 8A); in MNHN-Bol V 3348 (Fig. 4A), the nasals are strongly convex but with a narrow, anteriorly projecting median process.

The temporal fossa and the temporal lines are not clearly observable in all the specimens, owing to breakage and/or diagenetic deformation (Figs 6, 7). In general, the temporal lines appear straight and roughly parallel to one another, diverging anteriorly as they approach the postorbital processes of the frontal bones. The temporal lines curve laterally and ventrally at their posterior limit, extending parallel and slightly anterior to the nuchal crest (Figs 4, 5, 8).

In lateral view, the anterior part of the cranium is dominated by the maxilla. This bone contacts the nasal and the frontal dorsally, the lacrimal in its middle

part and the palatine and the alisphenoid posteriorly. The premaxillae are preserved in six specimens. They are V-shaped in MNHN-Bol V 3348, 3711 and 3726 (Figs 4C, 5C, 6C), whereas they show a more arched profile (and even flatten anteriorly as they approach their midline junction) in MNHN-Bol V 11731, 3717 and 3718 (Figs 2C, 7C, 8C). Their medial and lateral rami are nearly equivalent in size, with the lateral ramus slightly longer than the medial one, in MNHN-Bol V 3348, 3711 and 3726 (Figs 4C, 5C, 6C), whereas the lateral ramus is substantially longer than the medial ramus in MNHN-Bol V 11731, 3717 and 3718 (Figs 2C, 7C, 8C). The palate is rugose and strongly widened anteriorly, especially in MNHN-Bol V, 11731, 3321, 3717 and 3718 (Figs 2C, 3C, 7C, 8C); whereas it is narrower in MNHN-Bol V 3348, 3711 and 3726 (Figs 4C, 5C, 6C; see also 'Morphometric analyses' subsection below). In lateral view, the palate is concave at the level of Cf1–Mf1 and convex posteriorly at the level of Mf2–Mf4. The anterior palatal foramina (*sensu* De Iuliis *et al.*, 2011) are always clearly delineated (Figs 2C, 3C, 4C, 5C, 6C, 7C, 8C) and continue

8.90

8.95

8.100

8.105

8.110
8.111
8.112

Figure 5. A–D, cranium of *Simomylodon uccasamamensis* (MNHN-Bol V 3711) in dorsal (A), lateral (B), ventral (C) and posterior (D) views. E, isolated jugal in lateral view. F–H, mandibles in occlusal (F), ventral (G) and lateral (H) views. Scale bars: 5 cm.

into distinct anterior grooves that extend medially to connect with the incisive foramina (not visible in ventral view). Also, enlarged postpalatal foramina (*sensu* Gaudin, 2011) are observable in all specimens (Figs 2C, 3C, 4C, 5C, 6C, 7C, 8C).

The sphenorbital fissure and the optic and sphenopalatine foramina are visible in MNHN-Bol V 3711, 3717 and 3718 (Figs 5, 7, 8). These foramina open into a common depression and are approximately aligned horizontally. The sphenorbital fissure is the posteriormost and largest of the three foramina mentioned above. The optic foramen is adjacent to the sphenorbital fissure and the sphenopalatine foramen is farther anterior, at the anterior margin of the common depression. Posteriorly and ventrally, the foramen ovale is

located between the squamosal and the lateral plate of the pterygoid and opens onto the lateral wall of the cranium.

In ventral view, the structures of the middle region of the basicranium are difficult to observe, owing to poor preservation and complete fusion of the sutures. The pterygoids are inflated at their base (Fig. 5). The descending laminae of the pterygoid are broad and deep, but only preserved fully in MNHN-Bol V 3711 and 3717 (Figs 5, 7).

In lateral view, the lacrimal is more elongated anteroposteriorly than dorsoventrally and is pierced by a rounded lacrimal foramen. The orbital portion of the bone is larger than its facial portion. The jugal is firmly attached to the lacrimal and possesses

Figure 6. A–C, cranium and mandibles of *Simomylodon uccasamamensis* (MNHN-Bol V 3726) in dorsal (A), lateral (B) and ventral (C) views. D–F, mandibles in occlusal (D), lateral (E) and ventral (F) views. Scale bars: 5 cm.

ascending, descending and middle processes (Figs 5B, 6B, 7B, 8B), as is typical for sloths (Gaudin, 2004). The ascending process is the longest of the three. It is wide at its base, becoming narrower posteriorly, and ends as a rounded tip located at the level of the anteroposterior midpoint of the zygomatic process of the squamosal. The ascending and middle processes are strongly divergent in MNHN-Bol V 3717 and 3718 (Figs 7B, 8B) and more convergent in MNHN-Bol V 3711 and 3726 (Figs 5E, 6B). The ascending process of the jugal is marked by a weak postorbital process near its base (Figs 5E, 6B, 7B, 8B). The middle process of the jugal is triangular in shape and closely approaches the zygomatic process of the squamosal posteriorly. The descending process of the jugal bears a posteriorly or posteromedially extended hook in

MHNH-BOL V 3717 and 3718 (Figs 7, 8) that is not present in MNHN-Bol V 3711 and 3726 (Figs 5, 6). The long zygomatic process of the squamosal is almost horizontal in lateral view and anterolaterally directed in dorsal view (Figs 4–8).

In lateral view, the occipital is inclined anteriorly in MNHN-Bol V 3711 (Fig. 5B), whereas it appears more vertical in MNHN-Bol V 3718 (Fig. 8B). In posterior view (Fig. 5D), its transverse breadth exceeds its dorsoventral height. It is marked by a slight median external occipital crest that does not continue dorsally into a sagittal crest and culminates ventrally in a well-marked notch on the posterior edge of the foramen magnum (Fig. 5D). The nuchal crests are strongly developed and clearly visible in dorsal, lateral and posterior views (Figs 5, 8). The occipital condyles,

11.5
11.10
11.15
11.20
11.25
11.30
11.35
11.40
11.60
11.65
11.70
11.75
11.80
11.85
11.90
11.95
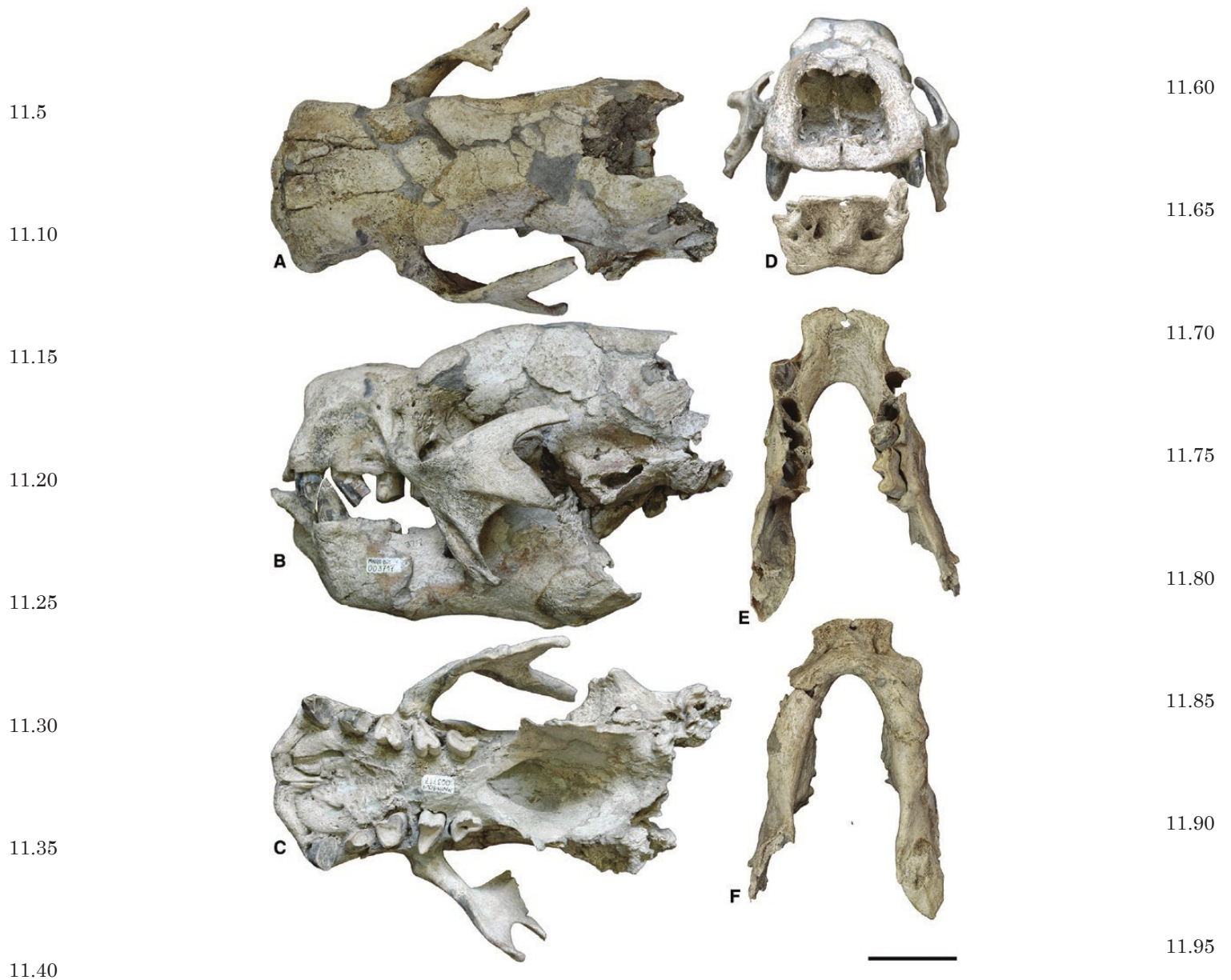
Figure 7. A–D, cranium and mandibles of *Simomylodon uccasamamensis* (MNHN-Bol V 3717) in dorsal (A), lateral (B), ventral (C) and anterior (D) views. E, F, mandibles in occlusal (E) and ventral (F) views. Scale bars: 5 cm.

11.45
11.50
11.55
11.56

in ventral view, are roughly triangular in shape, with a slightly concave medial edge, and are slightly more elongated mediolaterally than anteroposteriorly (Fig. 8C). In lateral view, they appear more prominent in MNHN-Bol V 3711 (Fig. 5B) than in MNHN-Bol V 3718 (Fig. 8B), a difference that is probably related to the inclination of the occiput already discussed.

Upper dentition: The upper tooth rows of *S. uccasamamensis*, composed of five teeth, are divergent anteriorly. The most mesial tooth is caniniform, whereas the remaining four are molariform

11.100
11.105
11.110
11.111
11.112

(Figs 4–8). There is no diastema between Cf1 and Mf1 (Figs 2–8). Cf1 is roughly semicircular in cross-section in most specimens: MNHN-Bol V 3711 and 3726 (Figs 5, 6), a shape that is also observable in the alveoli of MNHN-Bol V 11731 (Fig. 2). The straight side, corresponding ideally to the diameter of this semicircle, faces linguomesially, whereas the arched outline faces labiodistally. Variations of this shape are observable in the almost triangular caniniform of MNHN-Bol V 3717 (Fig. 7) and the nearly circular Cf1 (or correspondent alveoli) of MNHN-Bol V 3718 and 3321 (Figs 3, 8). In all the specimens where it is preserved, the occlusal

Figure 8. Cranium of *Simomylodon uccasamamensis* (MNHN-Bol V 3718) in dorsal (A), lateral (B) and ventral (C) views. Scale bar: 5 cm.

surface is almost vertical in lateral view and directed lingually and distally in occlusal view.

Mf1 is ovate in cross-section, elongated along the main axis of the tooth row. This tooth bears a lingual apicobasal sulcus in MNHN-Bol V 3718 (Fig. 8), absent in MNHN-Bol V 11371, 3321, 3711 and 3726 (Figs 2, 3, 5, 6). In MNHN-Bol V 3717 (Fig. 7), the lingual sulcus of Mf1 is slightly marked on the left and absent on the right, indicative of the great variability of this character. Mf1 bears a bevelled occlusal surface, with a mesial wear facet that is larger than the distal facet.

Mf2 and Mf3 are bilobate and exhibit a deep lingual apicobasal sulcus (Figs 3–8). In occlusal view, these two teeth are roughly triangular in cross-section, with the orthogonal angle disposed mesiolingually (Figs 3–8). Mf2 and Mf3 vary in their occlusal outlines, but Mf2 is generally longer mesiodistally than transversely, whereas in Mf3 the transverse width is equal to or exceeds the mesiodistal length. The wear facet of Mf2 is more pronounced distally than mesially, whereas in Mf3 it is more pronounced in the central part of the tooth than in its labial and lingual extremities (e.g. MNHN-Bol V 3711 and 3717; Figs 5, 7).

Mf4 is T-shaped in occlusal view, with the distal lobe clearly narrower transversely than the mesial one. The last upper tooth presents both lingual and labial longitudinal sulci, the latter more pronounced than the former (e.g. MNHN-Bol V 11731, 3321, 3711 and 3717; Figs 2, 3, 5, 7).

13.5

13.60

13.10

13.65

13.15

13.70

13.20

13.75

13.25

13.80

13.30

13.85

13.35

13.90

Figure 9. Left dentary of *Simomylodon uccasamamensis* (MNHN-Bol V 3296) in occlusal (A), lateral (B), ventral (C) and medial (D) views. Scale bar: 5 cm.

13.40

Mandible and lower dentition: The lower caniniform, like the upper one, is also generally semicircular in cross-section, with some exceptions represented by the triangular shape of MNHN-Bol V 3296 (Fig. 9A) and the ovate shape in MNHN-Bol V 3711 and 3371 (Figs 5F, 10D). It appears as the highest tooth of the lower tooth row and is nearly equal in size to mf1 (Figs 5–7, 9–12). The cf1 is bevelled, with the mesial wear facet broader than the distal one. It also presents a slight lingual apicobasal sulcus in MNHN-Bol V 3726 (Fig. 6), 3296 (Fig. 9) and the juvenile mandibles (Fig. 12), a feature not observable in the other specimens (Figs 5, 7, 10, 11).

13.45

13.50

A lingual apicobasal sulcus is a consistent feature of mf1. This tooth is transversely wider mesially than distally and bears an oblique, distally inclined wear facet (Figs 5–7, 9–12). The irregular cross-section of

13.55

13.56

mf2 resembles a parallelogram (Figs 5–7, 9–12). The presence of longitudinal sulci on this tooth is variable among the observed specimens. In MNHN-Bol V 3296 (Fig. 9), sulci are present on all four sides, whereas in MNHN-Bol V 3371 (Fig. 10D) they are almost absent. These two morphologies represent the extremes of the observable variation for mf2.

13.95

In occlusal view, mf3 is strongly bilobate, with the mesial lobe wider transversely than the distal lobe (Figs 5–7, 9, 10, 12). The mesial lobe is extended mesiolabially, with an apicobasal sulcus that faces mesiolingually. The distal lobe of mf3 is rounded distally. The two lobes are separated by a thin isthmus accompanied lingually by a deep, broad apicobasal sulcus, absent on the labial side (Figs 5–7, 9, 10, 12).

13.100

13.105

The mandible of *S. uccasamamensis* is short and deep, with the ventral border of the horizontal ramus

13.110

13.111

13.112
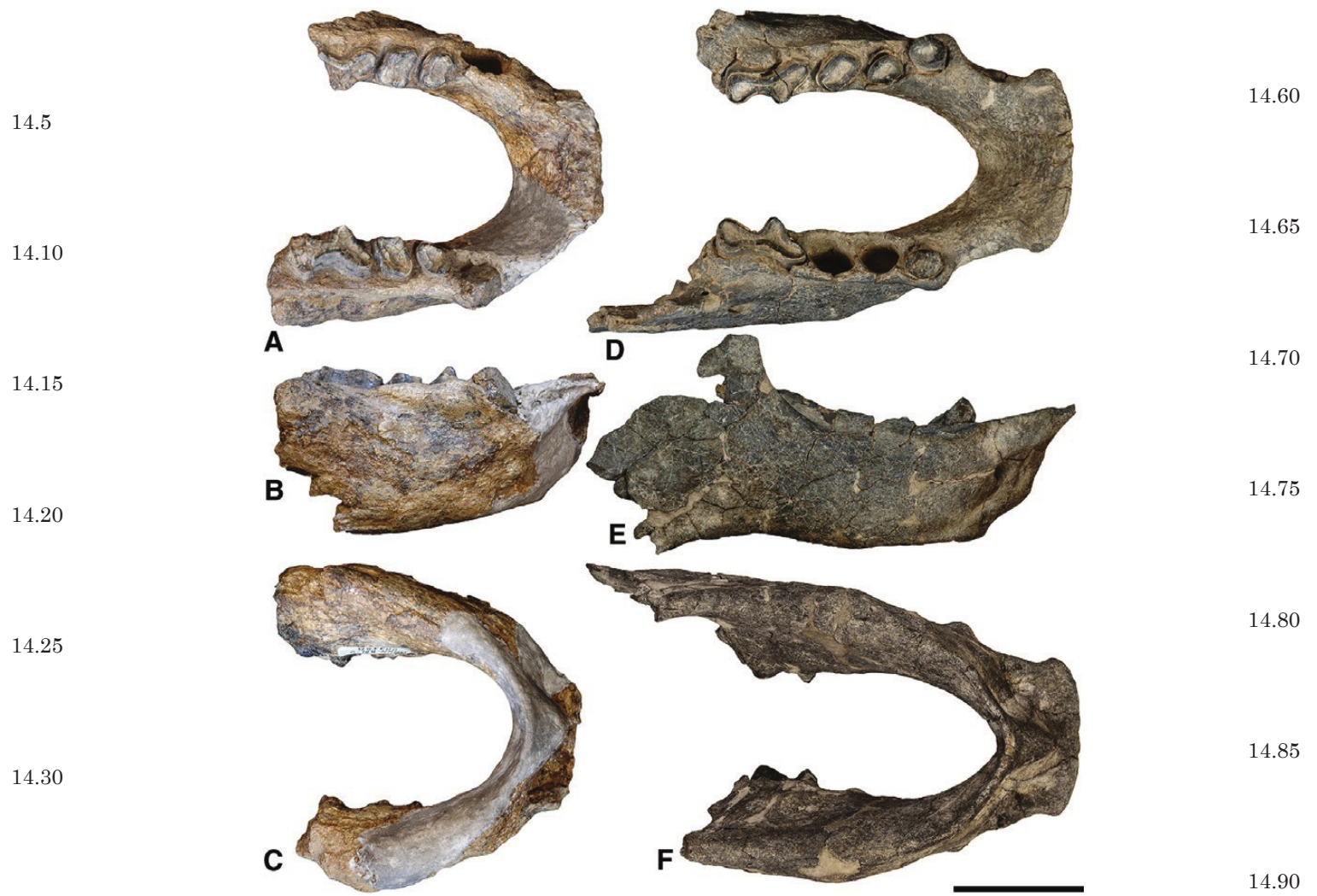
Figure 10. Mandibular fragments of *Simomylodon uccasamamensis* (A–C, MNHN-Bol V 3358; D–F, MNHN-Bol V 3371) in occlusal (A, D), lateral (B, E) and ventral (C, F) views. Scale bar: 5 cm.

nearly horizontal in lateral view (Figs 5–7, 9, 10, 12). The tooth row is aligned in occlusal view, with the exception of the cf1, which is slightly displaced laterally. The dorsoventral depth of the horizontal ramus of the mandible is constant along the tooth row, becoming narrower towards the symphyseal spout and deepening posteriorly at the base of the ascending ramus. The profile of the symphyseal spout in lateral view is irregular, with a strong convexity flanked by marked dorsal and ventral concavities (Figs 5–7, 9–11). In occlusal view, the symphysis is wider distally than proximally, with a visible constriction anterior to the caniniforms. The mandibular foramen is located on the medial side of the mandible, well posterior and slightly ventral to the base of mf3. The posteroexternal opening of the mandibular canal (a characteristic feature of

sloths among xenarthrans; see Gaudin, 2004; De Iuliis *et al.*, 2011) faces laterally at the level of the posterior edge of the root of mf3, well ventral to the dorsal edge of the horizontal ramus. The mandibular canal emerges anteriorly through the mental foramina situated on the anterolateral surface of the symphyseal spout. The mental foramina are highly variable in size and number (e.g. a single one in MNHN-Bol V 3296 and six in MNHN-Bol V 3298; Figs 9, 11A–C), even in the two dentaries of a single individual (e.g. MNHN-Bol V 3717, 3371).

On the ascending ramus, the angular, condyloid and coronoid processes are equally divergent (Fig. 9). The angular process is deeply concave medially, with a strongly convex ventral edge that is clearly demarcated from the ventral edge of the horizontal ramus (Fig. 9). The transverse width of
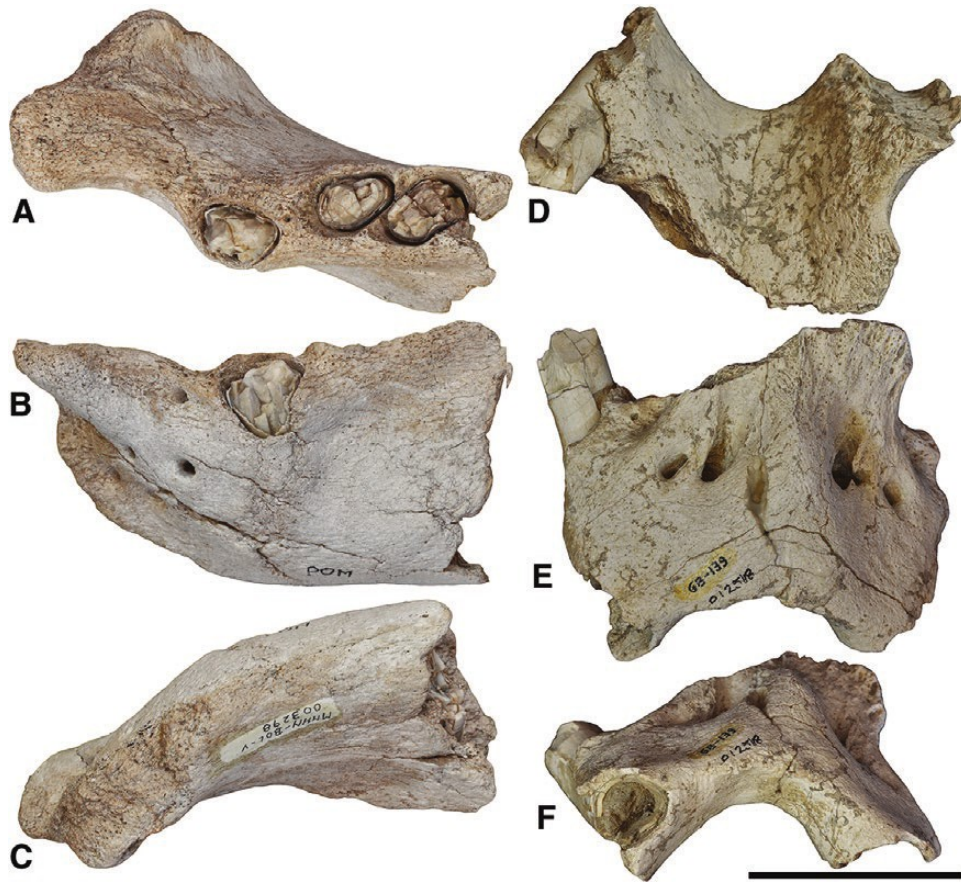
Figure 11. Left anterior mandibular corpus fragment of *Simomylodon uccasamamensis* (A–C, MNHN-Bol V 3298) in occlusal (A) lateral (B), and ventral (C) views, and anterior mandibular symphysis of *Simomylodon uccasamamensis* (D–F, MNHN-Bol V 12518) in occlusal (D), anterior (E) and ventral (F) views. Scale bar: 5 cm.

the mandibular condyle is much greater than its anteroposterior length. It has a hooked aspect in dorsal view, and its lateral portion is oriented horizontally in posterior view, whereas the medial portion is downturned ventrally. The coronoid process is tall, with its posterior edge orthogonal to the main mandibular axis in lateral view (Figs 6E, 9B, 12G). It is somewhat hooked posteriorly in MNHN-Bol V 3726 and 3359 (Figs 6E, 12G), but not in MNHN-Bol V 3296 (Fig. 9B). However, a complete coronoid process belonging to an adult individual is lacking in the present sample and therefore this feature cannot be assessed properly.

No important differences have been detected among the mandibular features of the specimens of *S. uccasamamensis*. In general, the mandibles MNHN-Bol V 3717, 3358 and 3298 (Figs 7, 10A–C, 11A–C) are more robust than the specimens MNHN-Bol V 3711, 3726, 3296, 3371 and 12518 (Figs 5, 6, 9, 10D–F, 11D–F). This greater robustness is exemplified by the two specimens MNHN-Bol V 3358 and 3371, illustrated

in Fig. 10, with the former (Fig. 10A–C) showing a more robust dentition and more anteriorly divergent, thicker and deeper horizontal rami than the latter (Fig. 10D–F). These variations were treated by Anaya & MacFadden (1995) as possible indicators of different ontogenetic stages and/or the existence of sexual dimorphism.

The *S. uccasamamensis* sample also includes four mandibular corpora of juvenile individuals (i.e. MNHN-Bol V 3359, 11758, 12001 and MNHN.F.AYO165; Fig. 12). In juvenile specimens of *Simomylodon*, cf1 is larger and wider than mf1–mf2, as in *Choloepus* (Hautier *et al.*, 2016) and *Glossotherium tropicorum* (De Iuliis *et al.*, 2017). The cf1 also shows a semicircular section and a feeble apicobasal sulcus in the lingual side (Fig. 12A–I). The mf1 and mf2 are somewhat more rounded and simple but already show the same occlusal pattern described above for adults. Additionally, mf3 already shows the same peculiar shape as the adult tooth, with a wide mesial and narrow distal lobe and the presence of a single lingual

16.5

16.10

16.15

16.20

16.25

16.30

16.35

16.40

16.60

16.65

16.70

16.75

16.80

16.85

16.90

16.95

Figure 12. Juvenile mandibular remains of *Simomylodon uccasamamensis*. A–C, left anterior mandibular fragment (MNHN-Bol V 12001) in lateral (A), occlusal (B) and medial (C) views. D–F, right mandibular fragment (MNHN.F.AYO165) in lateral (D), occlusal (E) and medial (F) views. G–I, left mandibular fragment with complete dentition (MNHN-Bol V 3359) in lateral (G), occlusal (H) and medial (I) views. J–L, right mandibular fragment (MNHN-Bol V 11758) in lateral (J), occlusal (K) and medial (L) views. Scale bar: 5 cm.

16.45

16.100

apicobasal sulcus (Fig. 12A–I). Also, the coronoid and condyloid processes appear simpler, without the small incisura on the posteriormost tip of the coronoid process (Fig. 12G–I). In posterior view, the condyle appears to be inclined laterally, rather than medially. Overall, the juvenile specimens of *S. uccasamamensis* already display the diagnostic features of the adults,

appearing largely as smaller scale versions of the adult bone.

Comparison

Cranium and upper dentition: In *S. uccasamamensis*, the presence of a high braincase, a deep and anteriorly elevated snout, and an approximately horizontal

16.50

AQ11

16.55

16.56

16.105

16.110

16.111

16.112

cranial base in lateral view are typical features of Mylodontidae (Gaudin, 2004). The width of the braincase relative to total skull length is comparable to *Pleurolestodon acutidens* (FMNH P14495; Rovereto, 1914) and is greater than *Glossotheridium chapadmalense*, *Glossotherium robustum*, *Mylodon darwinii* or *Paramylodon harlani* (Owen, 1842; Stock, 1925; Kraglievich, 1925, 1934; McAfee, 2009; Brandoni *et al.*, 2010).

Other features, above all in the rostral region, allow assignment of *Simomylodon* to the Mylodontinae. In particular, the snout is relatively short, widened anteriorly in dorsal view and depressed in lateral view (Figs 2, 4–8).

The wide rostrum of *S. uccasamamensis* is also accompanied by an anterior enlargement of the nasals. The nasal becomes narrower posteriorly and widens again at the level of the nasofrontal suture (Figs 2, 4–8). This expansion is a recurrent feature in mylodontids, as is the great enlargement of the external nares (Gaudin, 2004). The characters observed on the rostrum are closely related to the morphology of the palate. Indeed, *S. uccasamamensis* shows a V-shaped palate (Figs 2–8), comparable with all the mylodontines and lestodontines (Gaudin, 2004) except *Mylodon*, which has secondarily lost Cf1s, and consequently, reduced anterior palatal width (Kraglievich, 1934; Brandoni *et al.*, 2010). The medial anterior palatal processes of the maxilla are projected farther anteriorly than the lateral ones (Figs 2–8). This characteristic is also observed in *Glossotheridium*, *Glossotherium*, *Paramylodon*, *Pleurolestodon* and *Mylodon* (Owen, 1842; Rovereto, 1914; Stock, 1925; Kraglievich, 1925, 1934; McAfee, 2009; Brandoni *et al.*, 2010). The extension of the medial palatal processes of the maxilla is moderate anteroposteriorly, but the processes are broad mediolaterally (Figs 2–8). In this respect, *S. uccasamamensis* resembles more *Pleurolestodon acutidens* (FMNH P14495) than *Glossotheridium chapadmalense* (Kraglievich, 1925).

On the lateral cranial wall, the lacrimal is wide, with its orbital portion larger than its facial portion. The lacrimal is pierced by a small lacrimal foramen (Figs 4B, 7B), the diminutive size of this opening being a feature of all mylodontines and lestodontines (Gaudin, 2004).

All members of Mylodontidae are characterized by complex jugals with distinct ascending, descending and middle processes. The middle process is elongated and triangular, and the descending process is hooked posteriorly (Gaudin, 2004). All these features have been observed in the specimens attributed to *Simomylodon* (Figs 5B, 6B, 7B, 8B). Moreover, this taxon presents a weak postorbital process of the zygomatic arch, as in *Glossotheridium*,

Paramylodon, *Pleurolestodon* and the lestodontines (Kraglievich, 1925; Stock, 1925; Webb, 1989; Gaudin, 2004; McAfee, 2009). This is situated at the base of the ascending process, which is long and slender (Figs 5B, 6B, 7B, 8B), resembling that of *Glossotheridium*, *Glossotherium*, *Paramylodon* and *Mylodon* (Kraglievich, 1925, 1934; Stock, 1925; McAfee, 2009; Brandoni *et al.*, 2010). In contrast, *Pleurolestodon*, *Lestodon* and *Thinobadistes* have shorter and more robust ascending processes of the jugal (Rovereto, 1914; Webb, 1989; Bargo *et al.*, 2006). Finally, the ascending process of *S. uccasamamensis* is nearly horizontal, as in most mylodontids (Figs 5B, 6B, 7B, 8B; Gaudin, 2004).

The length of the zygomatic process of the squamosal is peculiar in *Simomylodon* because it is the longest (relative to the total cranial length) ever observed among mylodontids. Its almost horizontal orientation and its broad and flattened tip (Figs 4–8), however, are common features of mylodontines and lestodontines (Gaudin, 2004).

In dorsal view, the frontals and parietals are anteroposteriorly and mediolaterally flattened and the sagittal crest is absent (Figs 4–8). This morphology is present in all mylodontines and lestodontines except *Lestodon* (Gaudin, 2004). The presence of a flat temporal fossa, delimited by non-connecting temporal lines, is shared with *Pleurolestodon*, *Glossotherium*, *Paramylodon* and *Mylodon* (Owen, 1842; Rovereto, 1914; Stock, 1925; Kraglievich, 1934; McAfee, 2009; Brandoni *et al.*, 2010).

The strongly developed nuchal crest of constant width and aligned with the posterior surface of the occiput (this latter showing a median external occipital crest connecting the nuchal crest to the dorsal edge of the foramen magnum) are features of *Simomylodon* shared with all mylodontids (Gaudin, 2004). *Simomylodon* also exhibits a detached notch on the dorsal border of the foramen magnum, comparable with that observed in *Pleurolestodon* (FMNH P14495) and *Mylodon* (Kraglievich, 1934). In posterior view, the foramen magnum is limited laterally by roughly triangular occipital condyles. These lie at the level of the dentition in lateral view (Figs 5B, 8B). Both are common conditions in Mylodontidae (Gaudin, 2004). As in all mylodontines and lestodontines, the occipital condyles extend posteriorly to the posteriormost edge of the foramen magnum in ventral view (Figs 5C, 8C). The condyles are widely separated from one another, in this respect resembling *Glossotherium*, *Pleurolestodon* and *Thinobadistes*; also, they are mediolaterally elongated in ventral view to an extent that is comparable with *Mylodon*, *Pleurolestodon* and the lestodontines *Thinobadistes* and *Lestodon* (Owen, 1842; Rovereto, 1914; Stock,

1925; Kraglievich, 1934; Webb, 1989; McAfee, 2009; Brandoni *et al.*, 2010). In ventral view, the occipital condyles are well separated from the condyloid foramina (Figs 5C, 8C), as in *Pleurolestodon* (FMNH P14495).

The upper dentition of *S. uccasamamensis* is similar to the other representatives of Mylodontidae, with five teeth on each side aligned in two divergent tooth rows (Figs 2–8; Gaudin, 2004). Exceptions to this pattern are represented by Scelidotheriinae, which have parallel tooth rows (McDonald, 1987), and *Octomylodon* and *Mylodon*, which exhibit anterior tooth loss (Scillato-Yané, 1977; Brandoni *et al.*, 2010).

The Cf1–Mf1 diastema is absent or extremely reduced (Figs 5C, 8C), as in most mylodontids. Exceptions to this mylodontid pattern are represented by *Mylodon* and *Octomylodon* (Scillato-Yané, 1977; Brandoni *et al.*, 2010), in which Cf1 is secondarily lost, and *Lestodon*, which shows a derived and extremely elongated diastema (Czerwonogora & Fariña, 2013).

In *Simomylodon*, the most mesial upper tooth is strongly caniniform, as observed in all mylodontines and lestodontines, with the exception of *Pseudoprepotherium* (Hirschfeld, 1985). Cf1 is also the smallest of the upper tooth row (Figs 4–8), a feature in which *Simomylodon* closely resembles *Pleurolestodon*, *Glossotheridium*, *Glossotherium* and *Paramylodon* (Owen, 1842; Rovereto, 1914; Kraglievich, 1925; Stock, 1925; Robertson, 1976; McAfee, 2009). In occlusal view, Cf1 of *Simomylodon* is located at the anterior edge of the maxilla (Figs 2–8), as in *Pleurolestodon*, *Thinobadistes*, the megalonychid sloths and the extant *Bradypus* (Gaudin, 2004). The posterior curvature of Cf1 (Figs 2–8) is present in all mylodontines, whereas the alignment of both Cf1 and cf1 with the remainder of the tooth row is a feature of both mylodontines and scelidotheriines, although absent in *Lestodon* (McDonald, 1987; Gaudin, 2004; Czerwonogora & Fariña, 2013). The Cf1 of *S. uccasamamensis* exhibits almost vertical wear (Figs 5–7), like that found only in *Pleurolestodon acutidens* (FMNH P14495) among Neogene mylodontines. This feature is absent in *Paramylodon garbanii* (Robertson, 1976), *Glossotheriopsis pascuali* (Scillato-Yané, 1976) and *Glossotheridium chapadmalense* (Kraglievich, 1925).

Mf1 is also recurved posteriorly (Figs 3–7), as in several Mylodontidae but not in *Mylodon*, *Pseudoprepotherium*, *Lestodon* and Scelidotheriinae, where Mf1 is nearly straight (Gaudin, 2004). The ovate cross-section and the anteroposterior elongation of Mf1 observed in *Simomylodon* (Figs 2–8) is widespread in Mylodontidae, lacking only in *Octomylodon*, *Catonyx* and *Scelidotherium* (Scillato-Yané, 1977; Gaudin, 2004). Mf2 is longer mesiodistally than transversely, as is typical among mylodontines

and lestodontines. Mf2 and Mf3 present some peculiar features highly similar to the condition in *Pleurolestodon acutidens* and *Paramylodon garbanii*, such as their marked lingual sulcus and the almost orthogonal mesiolingual corner (Figs 3–7). In contrast, a marked lingual apicobasal sulcus is found only on Mf2, with a weak sulcus on Mf3, in *Glossotheridium chapadmalense* (Kraglievich, 1925). Finally, Mf4 is T-shaped (Figs 3–8), a peculiar feature of all members of the family Mylodontidae except *Octomylodon*, which possesses a bilobate Mf4 (Scillato-Yané, 1977; Gaudin, 2004).

Mandible and lower dentition: In occlusal view, cf1 is equivalent in size to mf1 (Figs 5–7, 9–12), and mf3 is the largest lower tooth, an invariant trait of Mylodontidae also known to occur in Bradypodidae (Gaudin, 2004). The cf1 is roughly semicircular in cross-section in most specimens, exceptionally displaying ovate or triangular cross-sections (Figs 5–7, 9–12). The latter two conformations are typical among Mylodontinae and Lestodontini, respectively (Gaudin, 2004). The caniniform of *Simomylodon* has a bevelled occlusal surface (Figs 5–7, 9, 10, 12), resembling that of *Pleurolestodon acutidens* (Rovereto, 1914) and *Paramylodon garbanii* (Robertson, 1976). The cf1 is bevelled also in *Glossotheridium chapadmalense*, but both wear facets are well developed in *Simomylodon* and *Pleurolestodon*, whereas the distal facet is extremely reduced in *Glossotheridium chapadmalense* (Kraglievich, 1925). Whereas cf1 of *Paramylodon garbanii* projects strongly mesially and labially (Robertson, 1976), that of *S. uccasamamensis* and *Glossotheridium chapadmalense* is implanted vertically (Kraglievich, 1925). The irregularly lobate mf1 and mf2 (Figs 5–7, 9–12) are very similar to those of *Pleurolestodon acutidens*, *Glossotheridium chapadmalense* and *Paramylodon garbanii*, but in *Simomylodon* they are significantly smaller in size. Moreover, *Paramylodon garbanii* shows deeper apicobasal sulci on the lingual and distal sides of mf2 (Robertson, 1976), whereas *Glossotheridium chapadmalense* has a more elongated and almost straight-walled mf2 (Kraglievich, 1925). The elongated and bilobate mf3 is a recurrent feature in Mylodontinae and Lestodontini (Gaudin, 2004). As already noted, mf3 has asymmetrically developed lingual and labial apicobasal sulci in *S. uccasamamensis*, with the former markedly deeper than the latter (Figs 5–7, 9, 10, 12). Among late Miocene–Pliocene Mylodontinae, the pattern of *S. uccasamamensis* is very similar to that of *Glossotheridium chapadmalense*, but differs from that of *Pleurolestodon acutidens* (FMNH P14495, 14521), in which both labial and lingual apicobasal sulci are well developed, and *Paramylodon*

garbanii (UF 10922), which displays an extra bulge on the labial side of mf3.

The mandible of *Simomylodon* presents some typical mylodontid features, such as the straight horizontal ventral edge of the horizontal ramus in lateral view, and a condyle located at the same level as the tooth row (Figs 5–7, 9, 10, 12) (Gaudin, 2004; Saint-André *et al.*, 2010). In general, the mandible of *Simomylodon* is smaller than that of all the other late Miocene–Pliocene mylodontids (i.e. *Pleurolestodon acutidens*, *Paramylodon garbanii* and *Glossotheridium chapadmalense*; Rovereto, 1914; Kraglievich, 1925; Robertson, 1976). The articular condyle of *Simomylodon* is convex and medially hooked in dorsal view, as in many Mylodontidae, in contrast to the condyle of lestodontines, which is extended both laterally and medially (Gaudin, 2004).

The angular process is the posteriormost process of the mandible (Fig. 9), another common mylodontid trait. Among Mylodontidae, only *Nematherium* and *Octomylodon* show an equally posterior extension of the condyloid process (Gaudin, 2004). In medial view, the mandible of *Simomylodon* shows a detached oblique ridge that extends from the anteroventral edge of the angular process towards the root of the last tooth (Fig. 9D). This last condition is shared with *Pleurolestodon*, *Glossotherium*, *Paramylodon* (Gaudin, 2004) and specimen MACN Pv 8675 of *Glossotheridium chapadmalense*. In lateral view, the ascending ramus does not cover mf3 (Figs 6E, 9B, 10E, 12D, G), resembling the condition observed in *Glossotheridium chapadmalense* and *Paramylodon garbanii* (Kraglievich, 1925; Robertson, 1976). This partial coverage of mf3 is observed in some other mylodontid genera, such as *Octodontotherium*, *Pseudoprepotherium*, *Mylodon* and *Pleurolestodon* (Gaudin, 2004). The anterior edge of the mandibular spout is broad and flat in occlusal view, as it is in *Glossotherium*, *Glossotheridium* and *Lestodon* (Owen, 1842; Kraglievich, 1925; McAfee, 2009; Czerwonogora & Fariña, 2013) (Figs 5–7, 9, 10). Other mylodontine genera, such as *Mylodon*, *Paramylodon* and *Pleurolestodon*, possess anteriorly rounded mandibular spouts (Stock, 1925; Kraglievich, 1934; McAfee, 2009; Brandoni *et al.*, 2010).

Four mandibles can be ascribed to juvenile individuals of *S. uccasamamensis*, based on their reduced size and lack of wear on the lower dentition (Fig. 12). These remains already display the main diagnostic features that have been found in the adults (e.g. a straight ventral margin, the absence of a diastema between cf1 and mf1, and the extreme reduction of the labial apicobasal sulcus on mf3; Fig. 12). All these features are in strong contrast to those observed in the juvenile mandibular fragment described by Oliva

& Brandoni (2012) and tentatively attributed to a 'mylodontid cf. *Simomylodon*' (Huayquerian SALMA, Buenos Aires Province, Argentina). The present data suggest that the specimen described by Oliva & Brandoni (2012) does not belong to *Simomylodon*, but rather is more compatible with the genus *Pleurolestodon*, also recognized in the Huayquerian SALMA of Argentina (Rovereto, 1914). However, given that no juvenile mandibular remains are known for that taxon, we prefer to consider the latter specimen as Mylodontinae indet.

morphometric analyses

The results of PCAs among the Neogene Mylodontinae are depicted in Figures 13 and 14, showing the two distinct modules: cranium and upper dentition (Fig. 13) vs. mandible and lower dentition (Fig. 14). We followed this approach in order to overcome the problem of the paucity of the data, thus maximizing the number of specimens that could be included in the analyses (for further details, see Material and Methods and Supporting Information, Appendix S5).

In the cranial dataset (Fig. 13), principal component (PC) 1 explains 51.80% of the variance and, given that all the variables have positive loadings, probably reflects body size. Size is lower on the left side and higher on the right. Principal component 2 (Fig. 13A) explains 17.42% of the variance. Positive values on this axis reflect skulls that have slender palates and thin rostra relative to total skull lengths, whereas negative values represent skulls with relatively wider palates and rostra. Finally, PC3 (Fig. 13B) explains 12.77% of the total variance. Positive values for PC3 are associated with robust dentitions and a long and deep snout relative to total skull lengths, whereas negative values are correlated with a reduced dental series and a short and slender snout (in relationship to total length). The Miocene–Pliocene sloths are well segregated along PC1 (Fig. 13), with *S. uccasamamensis* and *Glossotheriopsis pascuali* as the smallest taxa, and *Glossotheridium chapadmalense* as the largest taxon in the dataset. *Pleurolestodon acutidens* and *Paramylodon garbanii* occupy intermediate positions (Fig. 13).

On PC2, the extreme morphologies are represented by *Glossotheriopsis pascuali* in the positive range and *Paramylodon garbanii* in the negative range (Fig. 13A). However, these morphologies must be treated cautiously, because the result may be affected by the lack of total skull length measurements for both species, given that neither is represented by complete skulls. *Simomylodon* shows important variation along PC2, whereas *Pleurolestodon acutidens* and *Glossotheridium chapadmalense* do not overlap (Fig. 13A). This means that *Glossotheridium chapadmalense* exhibits a wider
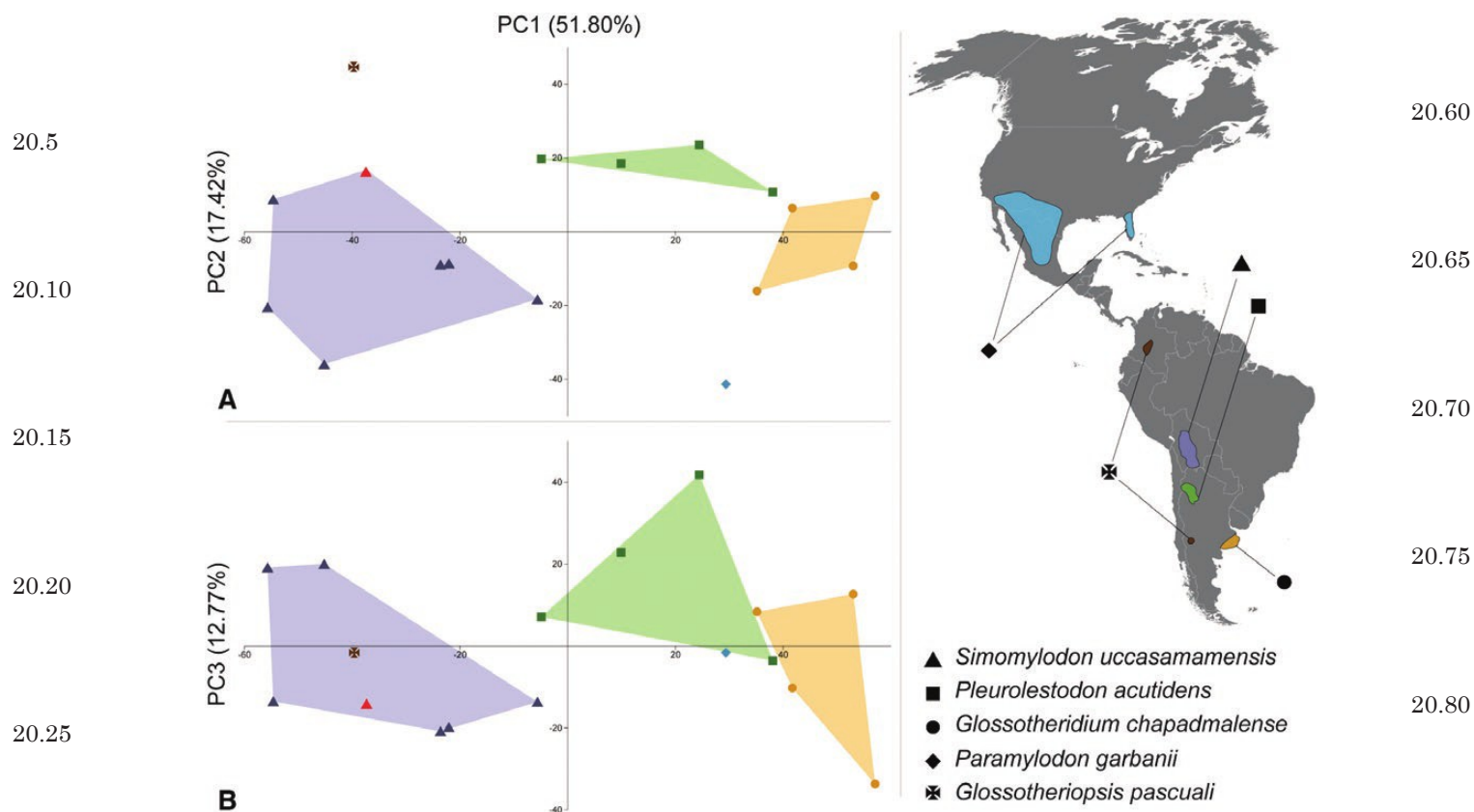
Figure 13. Principal components analysis performed on the cranial and upper dentition measurements subset (see Supporting Information, Appendix S5), showing the shape differentiation among the Miocene–Pliocene Mylodontinae. A, principal components 1 and 2; and B, principal components 1 and 3 (together explaining 81.99% of the among-group variance). On the right: associated palaeobiogeographical distribution of the taxa considered (for further information, see Supporting Information, Appendix S8).

palate and rostrum relative to total skull length than is the case for *Pleurolestodon acutidens*.

On PC3, *S. uccasamamensis* still shows high variation, including *Glossotheriopsis pascuali* from southern Argentina in its morphometric range (Fig. 13B). The most extreme morphologies are represented by *Pleurolestodon acutidens* (the highest values) and *Glossotheridium chapadmalense* (the lowest values). These two taxa, together with *Paramylodon garbanii*, partly overlap along PC3 (Fig. 13B).

In Fig. 13, the *S. uccasamamensis* specimen MNHN-Bol V 3348 (Fig. 3) is represented by a red triangle. This cranium was previously attributed to the species *Pleurolestodon dalenzae* by Saint-André *et al.* (2010). The present dataset shows that this specimen falls far outside the morphometric range of the genus *Pleurolestodon*, but well within the range of variation for *Simomylodon* (Fig. 13).

Likewise, a second PCA (Fig. 14) was performed on the variables of the mandible and lower dentition, yielding the same general pattern as the cranial analysis.

Principal component 1, which explains 57.96% of the total variance, is again a representation of size, and *Simomylodon* occupies the lowest positions on the left side of the graph (Fig. 14). *Glossotheridium chapadmalense* shows the largest mandibular values, whereas *Pleurolestodon acutidens* and *Paramylodon garbanii* are recovered in intermediate positions.

Principal component 2 explains 19.42% of the variance. Higher values are correlated with a long dental series and a deep mandibular ramus at the level of the dentition, relative to total mandibular length, whereas lower values correspond to a shorter dental series and less robust mandible.

Finally, PC3 explains 9.45% of the variance and reflects mandibles with a long horizontal ramus and anteroposteriorly narrow ascending ramus (positive values) vs. mandibles displaying a shorter horizontal ramus and a more anteroposteriorly enlarged ascending ramus (negative values).

On both PC1 and PC2 (Fig. 14A), *Simomylodon* shows the greatest range of variation, probably
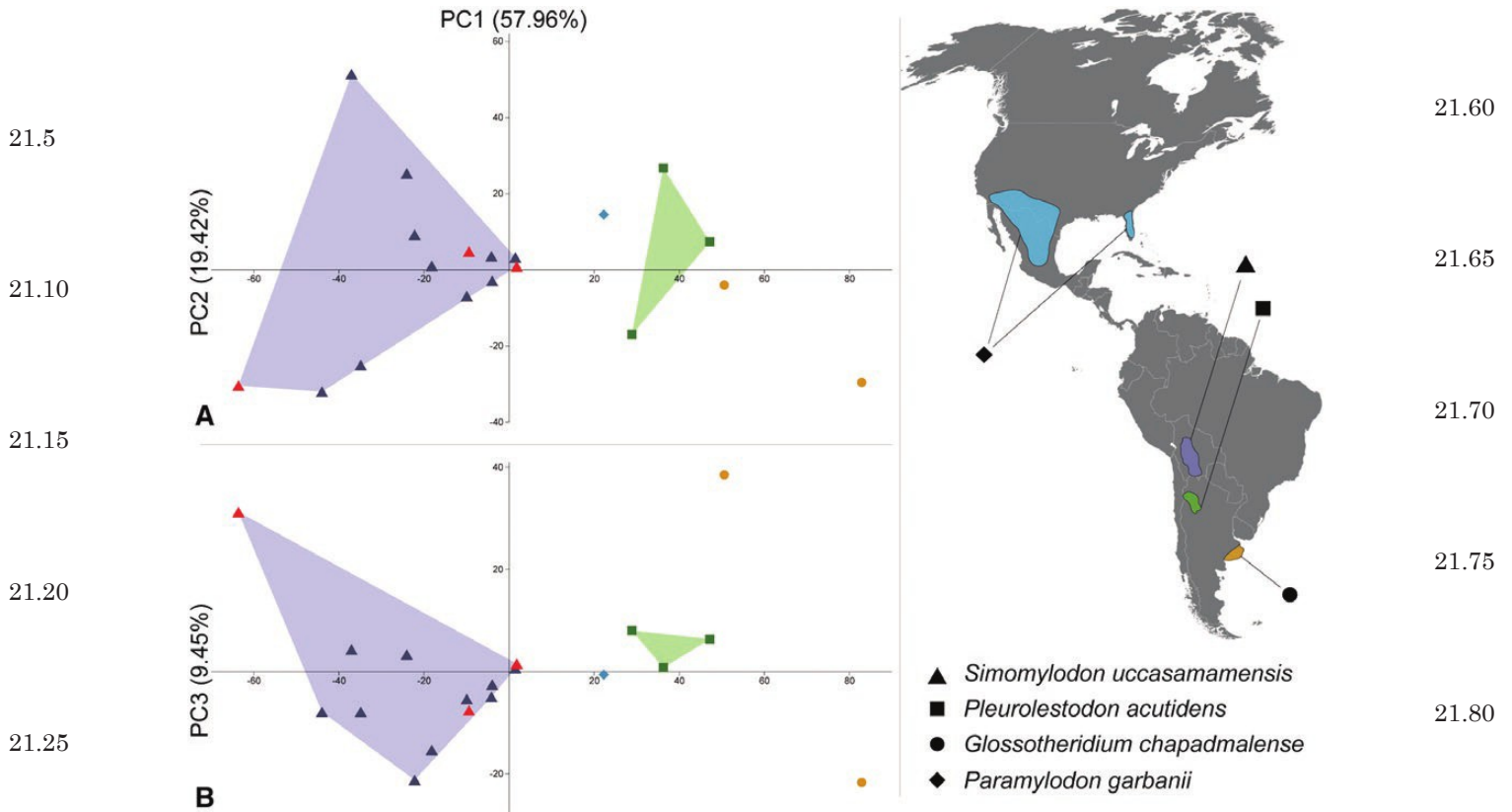
Figure 14. Principal components analysis performed on the mandibular and lower dentition measurements subset (see Supporting Information, Appendix S5), showing the shape differentiation among the Miocene–Pliocene Mylodontinae. A, principal components 1 and 2; and B, principal components 1 and 3 (together explaining 86.83% of the among-group variance). On the right: associated palaeobiogeographical distribution of the taxa considered (for further information, see Supporting Information, Appendix S8).

attributable to the inclusion of juvenile individuals in the dataset (Fig. 12). These specimens are retrieved in the far bottom-left portions of the graph depicting PC1 vs. PC2 (Fig. 14A), corresponding to the lowest values for both principal components. This means that they are the smallest specimens in the dataset (as expected), but they also possess a dental series that is reduced in length and horizontal rami that are of moderate depth relative to total mandibular length. *Glossotheridium chapadmalense* shows the highest variation on PC3 (Fig. 14B), an effect that is probably related to the incompleteness of the dataset for this taxon (no complete mandibles are known).

As before, the red triangles indicate the *S. uccasamamensis* specimens that were formerly assigned to another taxon. These are the specimens MNHN-Bol V 3358 (Fig. 10A–C), 3371 (Fig. 10D–F) and 3359 (Fig. 12G–I) that Anaya & MacFadden (1995) assigned to *Glossotheridium chapadmalense*. The more extensive data of the present analysis support their inclusion in the genus *Simomylodon* instead.

p hyloGenetic   analysis

The phylogenetic analysis recovered a single most parsimonious tree (tree length: 755 steps, : 0.662, R .927), with a topology compatible to that of the consensus tree from the analysis by Gaudin (2004). In our dataset, *Simomylodon* is deeply nested within Mylodontinae, more precisely as the sister taxon of the monospecific genus *Pleurolestodon* (Fig. 15). The node uniting the latter two taxa is well supported, with bootstrap and jackknife values of 53 and 70, respectively. These values are even greater than those supporting Mylodontinae (Supporting Information, Appendix S7). However, and in accordance with the previous study of Gaudin (2004), other groups are better supported, such as Lestodontini, Mylodontidae, Scelidotheriinae and Folivora (Supporting Information, Appendix S7).

The unambiguous synapomorphies that link *Simomylodon* and *Pleurolestodon* include: the Cf1 placed at the edge of the premaxilla (Gaudin, 2004:
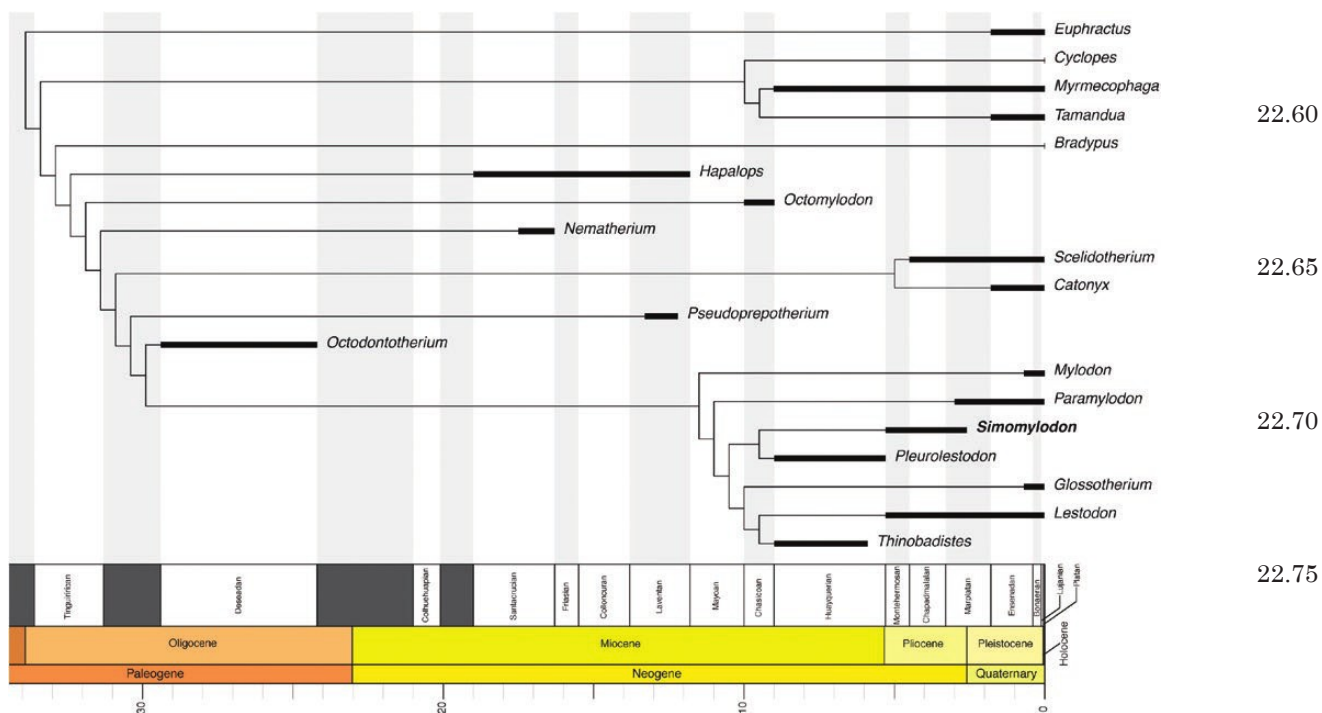
Figure 15. Most parsimonious tree (MPT) obtained from the phylogenetic analysis using TNT (tree length: 755 steps, CI = 0.662, RI = 0.927) and illustrated in chronostratigraphic context, following the known stratigraphic ranges of the taxa (for further information see Supporting Information, Appendix S8).

character 21, 1 → 0), the relatively wide braincase (Gaudin, 2004: character 82, 2→ 3) and the pronounced separation of the occipital condyles from the hypoglossal foramina (Gaudin, 2004: character 194, 1 → 2). The close morphological affinity of *Simomylodon* and *Pleurolestodon*, suggested by the present phylogenetic analysis, is probably the cause of the taxonomic misunderstanding of Saint-André *et al.* (2010), who assigned a gracile specimen of *Simomylodon* to a new species of *Pleurolestodon*.

Autapomophies of *S. uccasamamensis*, as retrieved by the present phylogenetic analyses are as follows: an intermediate shape of the coronoid process (Gaudin, 2004: character 47, 2 → 1), a posterodorsal inclination of the mandibular condyloid process in lateral view (Gaudin, 2004: character 52, 1 → 0), a short mandibular symphysis (Gaudin, 2004: character 62, 2→ 1), a weak buccinator fossa of the maxilla (Gaudin, 2004: character 106, 0→ 1), an ascending process of the jugal longer than the descending process (Gaudin, 2004: character 151, 0 → 1), a very elongate zygomatic process of the squamosal (Gaudin, 2004: character 168, 2 → 3), an enlarged condyloid foramen (Gaudin, 2004: character 187, 1 → 2) and a narrow and fairly deep mastoid depression (Gaudin, 1995: character 34, 1 → 0).

DISCUSSION

The new craniodental material of *S. uccasamamensis* includes several complete skulls and mandibles, which help us to assess morphological features previously unknown for this taxon. The new specimens provide information on anatomical areas that were missing in the specimens described by Saint-André *et al.* (2010), such as the cranial roof, the posterior portion and the lateral walls of the cranium, the jugals and several regions of the dentition.

Additionally, new specimens allow us to understand better the taxonomy of *Simomylodon* and *Pleurolestodon*. For example, the skull MNHN-Bol V 3348 (Fig. 3), considered by Saint-André *et al.* (2010) as the holotype of *Pleurolestodon dalenzae*, appears to be extremely similar in both shape and size to MNHN-Bol V 3711 (Fig. 5) and 3726 (Fig. 6). These two latter specimens preserve mandibular characters that are inconsistent with features of the genus *Pleurolestodon* (e.g. the flat anterior symphyseal spout in occlusal view and the lack of coverage of the mf3 by the ascending ramus in lateral view; Figs 5, 6; Rovereto, 1914). This hypothesis is further confirmed by the morphometric data. In fact, the genera *Simomylodon* and *Pleurolestodon* are clearly separated in both PCAs

(i.e. in both the cranial and mandibular data sub-sets; Figs 13, 14), revealing consistent differences in size and shape between the two taxa. For these reasons, the skull MNHN-Bol V 3348 from Choquecota (Fig. 3), previously attributed to *Pleurolestodon dalenzae* (Saint-André *et al.*, 2010), is here ascribed to the species *S. uccasamamensis* and represents the most ancient remains attributed to this species. Our morphological and morphometric data (Figs 13, 14) agree with the previous revision of Saint-André *et al.* (2010) regarding the existence, in the Neogene of Argentina, of a single species of the genus *Pleurolestodon* (i.e. *Pleurolestodon acutidens*).

The new enlarged cranial sample of *S. uccasamamensis* also allows us to assess intraspecific variation within this species. The morphology observed in this new material fills an anatomical gap between the specimens MNHN-Bol V 11731 and 3321 (Figs 2, 3) and MNHN-Bol V 3348 (Fig. 4), previously assigned to distinct species (Saint-André *et al.*, 2010). Moreover, Saint-André *et al.* (2010) stressed the strong similarity of MNHN-Bol V 3348 and the craniodental remains of *S. uccasamamensi*s. The phylogenetic analysis confirms the close relationship and associated morphological affinity of the genera *Pleurolestodon* and *Simomylodon* (Fig. 15).

Likewise, the *S. uccasamamensis* mandibular remains described here (Figs 5F–H, 6D–F, 7E–F, 9, 11, 12A–F, J–L) show the same features observed in mandibles from Inchasi described and illustrated by Anaya & MacFadden (1995: figs 3–5) (Figs 10, 12G–I). This is further supported by the morphometric data (Fig. 14), and therefore we have amended the assignment of the specimens MNHN-Bol V 3358 (Fig. 10A–C), 3371 (Fig. 10D–F) and 3359 (Fig. 12G–I) from *Glossotheridium chapadmalense* (Anaya & Macfadden, 1995) to *S. uccasamamensis*. The differences between the Pliocene Andean mylodontid (i.e. *Simomylodon*) and the southern genus *Glossotheridium* are also mentioned by Hoffstetter (1986). Moreover, differences between *Glossotheridium chapadmalense* from the Buenos Aires region (Kraglievich, 1925) and the North American species *Paramylodon garbanii* (Robertson, 1976) are recognized on both morphological and morphometric (Figs 13, 14) grounds, further confirming the taxonomic assignment of Morgan (2008) and McDonald & Morgan (2011).

Finally, the morphology observed in the mandibular sample of juvenile individuals (Fig. 12) from the present study is inconsistent with the juvenile mandibular corpus from the Huayquerian of Buenos Aires Province, tentatively placed in the genus *Simomylodon* by Oliva & Brandoni (2012). As a consequence, the geographical distribution of *S. uccasamamensis* is, for the moment, strictly limited to the Bolivian Altiplano.

This species can therefore be considered endemic to the Andes, reinforcing the biogeographical assertions of Saint-André *et al.* (2010).

Mylodontid remains are extremely rare in the Bolivian Altiplano before the Huayquerian–Montehermosan transition (Saint-André *et al.*, 2010). *Simomylodon uccasamamensis* appears for the first time slightly before the Miocene–Pliocene transition, in the Choquecota deposits, and it persists at several localities from the Altiplano until the late Pliocene, the last occurrence being at Ayo Ayo–Viscachani (Saint-André, 1994; Saint-André *et al.*, 2010). Chronologically, the presence of *S. uccasamamensis* in the Bolivian Altiplano encompasses two faunal turnover events that are particularly evident in the Bolivian deposits (Hoffstetter, 1986). The former occurred at the Miocene–Pliocene boundary and is coeval with the Quechua tectonic phase (Steinmann, 1929). It consisted of a folding event, associated with strong volcanic activity, that brought about an uplift of the Altiplano and resulted in drastic ecological changes, namely drier and colder environments than those of the late Miocene (e.g. Marshall *et al.*, 1983; Hoffstetter, 1986; Marshall & Sempéré, 1991; Saint-André, 1994; Saint-André *et al.*, 2010). The late Miocene fauna, dominated by the mesotheriids (e.g. *Plesiotypotherium*) and toxodontid notoungulates, is replaced by a Pliocene assemblage, with macraucheniid litopterns (cf. *Promacrauchenia*), the xotodontine notoungulate *Posnanskytherium*, large hydrochoerid rodents (e.g. *Chapalmatherium*) and several armoured xenarthrans, including sclerocalyptine glyptodonts, pampatheriine armadillos and megatheriid and mylodontid sloths (Marshall *et al.*, 1983; Hoffstetter, 1986). The younger and more dramatic faunal turnover in the Bolivian highlands occurred by the Pliocene–Pleistocene transition (~2.58 Mya) and was driven by the increasing influx of North American immigrants and a further rise of the Andes (e.g. Marshall *et al.*, 1983; Hoffstetter, 1986; Marshall & Sempéré, 1991). This event ended the isolation of the Pliocene faunas of the Altiplano, in which no North American immigrants have been reported to date (Anaya & MacFadden, 1995). The chronological distribution of *S. uccasamamensis* is bracketed between these two major faunal turnover events. During the Pliocene, the central Andes had already attained an elevation of 2000–2850 m (MacFadden *et al.*, 1994; Saint-André, 1994; Saint-André *et al.*, 2010) and probably acted as a faunal refuge or an 'Andean island'. The existence of such a refugium is indicated by the absence of North American immigrants from the Bolivian Altiplano, despite the fact that these immigrants have been reported from a number of more southerly localities in

Argentina during the Huayquerian, Montehermosan and Chapadmalalan SALMAs (Marshall *et al.*, 1983). Therefore, *S. uccasamamensis* might have been specifically adapted for the ecological conditions on the Bolivian Altiplano in the Pliocene, i.e. an isolated, cold and dry environment.

C onclusions

1. The moderate-sized Miocene–Pliocene mylodontids (i.e. *Glossotheridium chapadmalense*, *Glossotheriopsis pascuali*, *Paramylodon garbanii*, *Pleurolestodon acutidens* and *Simomylodon uccasamamensis*) can be separated both morphologically and morphometrically.
2. *Simomylodon uccasamamensis* and the poorly known *Glossotheriopsis pascuali* are smaller in size than *Glossotheridium chapadmalense*, *Paramylodon garbanii* and *Pleurolestodon acutidens*.
3. *Glossotheridium chapadmalense* and *Paramylodon garbanii*, from the Chapadmalalan SALMA of South America and the Late Blancan NALMA of North America, respectively, can be differentiated reliably on both morphological and morphometric grounds, following the assertions of Morgan (2008) and McDonald & Morgan (2011).
4. The species *Pleurolestodon dalenzae* (Saint-André *et al.*, 2010) is considered a junior synonym of *Simomylodon uccasamamensis*. The genus *Pleurolestodon* is therefore monospecific, with the Argentinean species *Pleurolestodon acutidens* as the only valid species recognized to date.
5. The mandibular fragments from Inchasi and assigned to *Glossotheridium chapadmalense* by Anaya & MacFadden (1995) are extremely similar to those of *S. uccasamamensis* in both shape and size, and therefore assigned to the latter species.
6. The juvenile mylodontid mandible from the Huayquerian SALMA of the Buenos Aires region was erroneously identified as 'cf. *Simomylodon*' by Oliva & Brandoni (2012); it does not possess the diagnostic features of the juvenile *S. uccasamamensis* specimens from Bolivia.
7. The phylogenetic analysis based on 286 craniodental features supported the morphological affinity of the genera *Pleurolestodon* and *Simomylodon*.
8. *Simomylodon uccasamamensis* is, to date, the only recognized mylodontid sloth from the Pliocene deposits of the Bolivian Altiplano. This species is endemic to this region during the Montehermosan, Chapdamalalan and (early) Marplatan SALMAs.
9. *Simomylodon uccasamamensis* may have been specifically adapted to the ecological conditions

that prevailed in the isolated, cold and dry ecosystems of the Bolivian Altiplano during the Pliocene epoch, without competition or predation from North American immigrants.

ACKNOWLEDGEMENTS

REFERENCES

Ameghino F. 1902. Notas sobre algunos mamiferos fosiles, nuevos ó poco conocidos del valle de Tarija. *Anales del Museo de Historia Natural de Buenos Aires* **8:** 225–261.

Anaya F, MacFadden BJ. 1995. Pliocene mammals from Inchasi, Bolivia: the endemic fauna just before the Great American Interchange. *Bulletin of the Florida Museum of Natural History* **39:** 87–140.

Anaya F, Pachero J, Pili LA. 1989. Hallazgo de mesotherinos en la formación Kasira (Terciario) en el Sud Boliviano, Prov. Modesto Omiste – Dpto. Potosí. *Boletín del Servicio Geológico de Bolivia* **4:** 41–46.

Bapst DW. 2012. paleotree: an R package for paleontological and phylogenetic analyses of evolution. *Methods in Ecology and Evolution* **3:** 803–807.

Bargo MS, Toledo N, Vizcaíno SF. 2006. Muzzle of South American Pleistocene ground sloths (Xenarthra, Tardigrada). *Journal of Morphology* **267:** 248–263.

24.5
24.10
24.15
24.20
24.25
24.30
24.35
24.40
24.45
24.50
24.55
24.56
24.60
24.65
24.70
24.75
24.80
24.85
AQ17
AQ18
24.90
24.95
24.100
24.105
24.110
24.111
24.112

Bargo MS, Vizcaíno SF. 2008. Paleobiology of Pleistocene ground sloths (Xenarthra, Tardigrada): biomechanics, morphogeometry and ecomorphology applied to the masticatory apparatus. *Ameghiniana* **45:** 175–196.

Bell MA, Lloyd GT. 2015. strap: an R package for plotting phylogenies against stratigraphy and assessing their stratigraphic congruence. *Palaeontology* **58:** 379–389.

Boule M, Thévenin A. 1920. *Mammifères fossiles de Tarija.* Paris: Imprimerie nationale.

Brandoni D, Ferrero BS, Brunetto A. 2010. *Mylodon darwini* Owen (Xenarthra, Mylodontidae) from the Late Pleistocene of Mesopotamia, Argentina, with remarks on individual variability, paleobiology, paleobiogeography, and paleoenvironment. *Journal of Vertebrate Paleontology* **30:** 1547–1558.

Bremer K. 1994. Branch support and tree stability. *Cladistics* **10:** 295–304.

Cattoi NV. 1966. Edentata. In: Borrello AV, ed. *Paleontografia Bonaerense*. La Plata: Comisión de Investigaciones Científicas de La Provincia de Buenos Aires, 59–99.

Cerdeño E, Vera B, Schmidt GI, Pujos F, Quispe BM. 2012. An almost complete skeleton of a new Mesotheriidae (Notoungulata) from the Late Miocene of Casira, Bolivia. *Journal of Systematic Palaeontology* **10:** 341–360.

Cione AL, Tonni EP. 1996. Reassesment of the Pliocene–Pleistocene continental time scale of Southern South America. Correlation of the type Chapadmalalan with Bolivian sections. *Journal of South American Earth Sciences* **9:** 221–236.

Coltorti M, Abbazzi L, Ferretti MP, Iacumin P, Rios FP, Pellegrini M, Pieruccini P, Rustioni M, Tito G, Rook L. 2007. Last Glacial mammals in South America: a new scenario from the Tarija Basin (Bolivia). *Die Naturwissenschaften* **94:** 288–299.

Croft DA. 2007. The middle Miocene (Laventan) Quebrada Honda fauna, Southern Bolivia and a description of its notoungulates. *Palaeontology* **50:** 277–303.

Czerwonogora A, Fariña RA. 2013. How many Pleistocene species of *Lestodon* (Mammalia, Xenarthra, Tardigrada)? *Journal of Systematic Palaeontology* **11:** 251–263.

De Iuliis G, Cartelle C, McDonald HG, Pujos F. 2017. The mylodontine ground sloth *Glossotherium tropicorum* from the late Pleistocene of Ecuador and Peru. *Papers in Palaeontology* **3:** 613–636.

De Iuliis G, Gaudin TJ, Vicars M. 2011. A new genus and species of nothrotheriid sloth (Xenarthra, Tardigrada, Nothrotheriidae) from the late Miocene (Huayquerian) of Peru. *Palaeontology* **54:** 171–205.

Delsuc F, Catzeflis FM, Stanhope MJ, Douzery EJP. 2001. The evolution of armadillos, anteaters and sloths depicted by nuclear and mitochondrial phylogenies: implications for the status of the enigmatic fossil *Eurotamandua*. *Proceedings of the Royal Society B: Biological Sciences* **268:** 1605–1615.

Esteban GI. 1996. *Revisión de los Mylodontinae cuaternarios (Edentata-Tardigrada) de Argentina, Bolivia y Uruguay. Sistemática, filogenia, paleobiología, paleozoogeografía y paleoecología.* Unpublished D. Phil. Thesis, Universidad Nacional de Tucumán.

Evernden JF, Kriz SJ, Cherroni C. 1966. Correlaciones de las formaciones terciarias de la cuenca altiplánica a base de edades absolutas, determinadas por el método potasio-argón. *Servicio Geológico de Bolivia, Hoja Informativa* **1:** 10–12.

Evernden JF, Kriz SJ, Cherroni C. 1977. Potassium-argon ages of some Bolivian rocks. *Economic Geology* **72:** 1042–1061.

Fariña RA, Vizcaíno SF. 2003. Slow moving or browsers? A note on nomenclature. *Senckenbergiana Biologica* **83:** 3–4.

Farris JS, Albert VA, Källersjö M, Lipscomb D, Kluge AG. 1996. Parsimony jackknifing outperforms neighbor-joining. *Cladistics* **12:** 99–124.

Felsenstein J. 1985. Confidence limits on phylogenies: an approach using the bootstrap. *Evolution* **39:** 783–791.

Flynn JJ, Swisher CC III. 1995. Cenozoic South American Land Mammal Ages: correlations to global geochronologies. *Geochronology, Time Scales and Global Stratigraphic Correlation, SEPM Special Publication* **54:** 317–333.

Gaudin TJ. 1995. The ear region of edentates and the phylogeny of the Tardigrada (Mammalia, Xenarthra). *Journal of Vertebrate Paleontology* **15:** 672–705.

Gaudin TJ. 2004. Phylogenetic relationships among sloths (Mammalia, Xenarthra, Tardigrada): the craniodental evidence. *Zoological Journal of the Linnean Society* **140:** 255–305.

Gaudin TJ. 2011. On the osteology of the auditory region and orbital wall in the extinct West Indian sloth genus *Neocnus* Arredondo, 1961 (Placentalia, Xenarthra, Megalonychidae). *Annals of Carnegie Museum* **80:** 5–28.

Gaudin TJ, Croft DA. 2015. Paleogene Xenarthra and the evolution of South American mammals. *Journal of Mammalogy* **96:** 622–634.

Gelfo JN, Goin FJ, Woodburne MO, de Muizon C. 2009. Biochronological relationships of the earliest South American Paleogene mammalian faunas. *Palaeontology* **52:** 251–269.

Goloboff P, Farris J, Nixon K. 2008. TNT, a free program for phylogeny analysis. *Cladistics* **24:** 774–786.

Hammer Ø, Harper DAT, Ryan PD. 2001. PAST: paleontological statistics software package for education and data analysis. *Palaeontología Electronica* **4:** art. 4.

Hautier L, Gomes Rodrigues H, Billet G, Asher RJ. 2016. The hidden teeth of sloths: evolutionary vestiges and the development of a simplified dentition. *Scientific Reports* **6:** 27763.

Hirschfeld SE. 1985. Ground sloths form the Friasian La Venta Fauna, with additions to the Pre-Friasian Coyaima Fauna of Colombia, South America. *University of California Publications in Geological Sciences* **128:** 1–91.

Hoffstetter R. 1956. Contribution à l'étude des Orophodontoidea, Gravigrades cuirassés de la Patagonie. *Annales de Paléontologie* **42:** 27–64.

Hoffstetter R. 1963. Note préliminaire sur la faune pléistocène de Tarija (Bolivie). *Bulletin du Muséum National d'Histoire Naturelle* **35:** 194–203.

Hoffstetter R. 1968. Un gisement de mammifères déséadiens (Oligocène inférieur) en Bolivie. *Compte Rendu de l'Académie des Sciences* **267:** 1095–1097.

Hoffstetter R. 1977. Un gisement de mammifères miocènes à Quebrada Honda (sud bolivien). *Compte Rendu de l'Académie des Sciences* **285:** 1517–1520.

Hoffstetter R. 1986. High Andean mammalian faunas during the Plio-Pleistocene. In: Vuilleumier F, Monasterio M, eds. *High altitude tropical biogeography*. New York: Oxford University Press, 219–245.

Hoffstetter R, Martínez C, Mattauer M, Tomasi P. 1971a. Lacayani, un nouveau gisement bolivien de mammifères déséadiens (Oligocène inférieur). *Compte Rendu de l'Académie des Sciences* **273:** 2215–2218.

Hoffstetter R, Martínez C, Muñoz-Reyes J, Tomasi P. 1971b. Le gisement d'Ayo Ayo (Bolivie), une succession stratigraphique Pliocène–Pléistocène datée par des mammifères. *Comptes Rendus de l'Académie des Sciences* **273:** 2472–2475.

Hoffstetter R, Martínez C, Tomasi P. 1972. Nouveaux gisements de mammifères néogènes dans les couches rouges de l'Altiplano bolivien. *Compte Rendu de l'Académie des Sciences* **275:** 739–742.

International Commission on Zoological Nomenclature (ICZN). 1999. *International code of zoological nomenclature, 4th edition*. London: The International Trust for Zoological Nomenclature.

Kraglievich L. 1921. Estudios sobre los Mylodontinae. Descripción comparativa del genero "*Pleurolestodon*" Rov. *Anales del Museo Nacional de Historia Natural de Buenos Aires* **31:** 95–118.

Kraglievich L. 1925. Cuatro nuevos Gravigrados de la fauna araucana chapadmalense. *Anales del Museo Nacional de Historia Natural "Bernardino Rivadavia"* **33:** 215–235.

Kraglievich L. 1934. Contribución al conocimiento de "*Mylodon darwini*" Owen y especies afines. *Revista del Museo de la Plata* **34:** 255–292.

Lavenu A. 1984. Age pliocène de la formation Remedios, dans l'Altiplano bolivien: caractères de la tectonique pliocène. *Comptes Rendus de l'Académie des Sciences* **299:** 1051–1054.

Lavenu A, Bonhomme MG, Vatin-Perignon N, De Pachtere P. 1989. Neogene magmatism in the Bolivian Andes between 16°S and 18°S: stratigraphy and K/Ar geochronology. *Journal of South American Earth Sciences* **2:** 35–47.

MacFadden BJ, Anaya F, Argollo J. 1993. Magnetic polarity stratigraphy of Inchasi: a Pliocene mammal-bearing locality from the Bolivian Andes deposited just before the Great American Biotic Interchange. *Earth and Planetary Science Letters* **114:** 229–241.

MacFadden BJ, Siles O, Zeitler P, Johnson NM, Campbell JKE. 1983. Magnetic polarity stratigraphy of the middle Pleistocene (Ensenadan) Tarija Formation of Southern Bolivia. *Quaternary Research* **19:** 172–187.

MacFadden BJ, Wang Y, Cerling TE, Anaya F. 1994. South American fossil mammals and carbon istotopes: a 25 million-year sequence from the Bolivian Andes. *Palaeogeography, Palaeoclimatology, Palaeoecology* **107:** 257–268.

MacFadden BJ, Zeitler PK, Anaya F, Cottle JM. 2013. Middle Pleistocene age of the fossiliferous sedimentary sequence from Tarija, Bolivia. *Quaternary Research* **79:** 268–273.

Maddison WP, Maddison DR. 2011. *Mesquite: a modular system for evolutionary analysis*, *Version 3.04*. Available at: http://mesquiteproject.org/

Marshall LG, Hoffstetter R, Pascual R. 1983. Mammals and stratigraphy: geochronology of the continental mammal-bearing Tertiary of South America. *Palaeovertebrata (Mémoire Extraordinaire)*: 1–76.

Marshall LG, Sempéré T. 1991. The Eocene to Pleistocene vertebrates of Bolivia and their stratigraphic context: a review. In: Suárez-Sorouco R, ed. *Fósiles y Facies de Bolivia*, **Vol. I**, *Vertebrados*. Santa Cruz: *Revista Técnica de YPFB*, **12:** 631–652.

Marshall LG, Swisher CC, Lavenu A, Hoffstetter R, Curtis GH. 1992. Geochronology of the mammal-bearing late Cenozoic on the northern Altiplano, Bolivia. *Journal of South American Earth Sciences* **5:** 1–19.

McAfee RK. 2009. Reassessment of the cranial characters of *Glossotherium* and *Paramylodon* (Mammalia: Xenarthra: Mylodontidae). *Zoological Journal of the Linnean Society* **155:** 885–903.

McDonald HG. 1987. *A systematic review of the Plio-Pleistocene scelidotheriine ground sloths (Mammalia: Xenarthra: Mylodontidae)*. Unpublished D. Phil. Thesis, University of Toronto.

McDonald HG. 1997. Xenarthrans: Pilosans. In: Kay RF, Madden RH, Cifelli RL, Flynn JJ, eds. *Vertebrate paleontology in the Neotropics. The Miocene fauna of La Venta, Colombia*. Washington and London: Smithsonian Institution Press, 233–245.

McDonald HG, De Iuliis G. 2008. Fossil history of sloths. In: Vizcaíno SF, Loughry WJ, eds. *The biology of the Xenarthra*. Gainesville: University Press of Florida, 39–55.

McDonald HG, Morgan GS. 2011. Ground sloths of New Mexico. *New Mexico Museum of Natural History and Science Bulletin* **53:** 652–663.

McKenna MC, Bell SK. 1997. *Classification of mammals above the species level*. New York: Columbia University Press.

Mones A. 1986. Palaeovertebrata sudamericana. Catálogo sistemático de los vertebrados fósiles de America del Sur – Parte I. Lista preliminar y bibliografía. *Courier Forschungsinstitut Senckenberg* **82:** 1–625.

Montellano-Ballesteros M, Carranza-Castañeda Ó. 1986. Descripción de un milodóntido del Blancano temprano de La Mesa Central de México. *Universidad Nacional Autónoma de Mexico, Instituto de Geología, Revista* **6:** 193–203.

Morgan GS. 2008. Vertebrate fauna and geochronology of the Great American Biotic Interchange in North America. In: Lucas SG, Mogan GS, Spielmann JA, Prothero DR, eds. *Neogene Mammals. Bulletin of the New Mexico Museum of Natural History and Science* **44:** 93–140.

AQ22 **de Muizon C. 1991.** La fauna de mamíferos de Tiupampa (Paleoceno inferior, Formación Santa Lucia), Bolivia. In: Suárez-Sorouco R, ed. *Fósiles y Facies de Bolivia, Vol. I, Vertebrados*. Santa Cruz: *Revista Técnica de YPFB* **12:** 575–624.

de Muizon C. 1999. Marsupial skulls from the Deseadan (late Oligocene) of Bolivia and phylogenetic analysis of the Borhyaenoidea (Marsupialia, Mammalia). *Geobios* **32:** 483–509.

Oliva C, Brandoni D. 2012. Primer registro de Mylodontinae (Tardigrada, Mylodontidae) en el Huayqueriense (Mioceno tardío) de la provincia de Buenos Aires, Argentina. *Revista del Museo Argentino de Ciencias Naturales* **14:** 325–332.

Owen R. 1842. *Description of the skeleton of an extinct gigantic sloth,* Mylodon *robustus, Owen, with observations on the osteology, natural affinities, and probable habits of the megatheroid quadrupeds in general*. London: Direction of the Council.

AQ23 **Pitana VG, Esteban GI, Ribeiro AM, Cartelle C. 2013.** Cranial and dental studies of *Glossotherium robustum* (Owen, 1842) (Xenarthra: Pilosa: Mylodontidae) from the Pleistocene of southern Brazil. *Alcheringa* **37:** 147–162.

Pujos F, De Iuliis G. 2007. Late Oligocene Megatherioidea fauna (Mammalia: Xenarthra) from Salla-Luribay (Bolivia): new data on basal sloth radiation and Cingulata-Phyllophaga split. *Journal of Vertebrate Paleontology* **27:** 132–144.

Pujos F, De Iuliis G, Cartelle C. 2017. A paleogeographic overview of tropical fossil sloths: towards an understanding of the origin of extant suspensory sloths? *Journal of Mammalian Evolution* **24:** 19–38.

Pujos F, De Iuliis G, Mamani Quispe B. 2011. *Hiskatherium saintandrei*, gen. et sp. nov.: an unusual sloth from the Santacrucian of Quebrada Honda (Bolivia) and an overview of middle Miocene, small megatherioids. *Journal of Vertebrate Paleontology* **31:** 1131–1149.

Pujos F, De Iuliis G, Mamani Quispe B, Adnet S, Andrade Flores R, Billet G, Fernández-Monescillo M, Marivaux L, Munch P, Prámparo MB, Antoine P-O. 2016. A new nothrotheriid xenarthran from the early Pliocene of Pomata-Ayte (Bolivia): new insights into the caniniform–molariform transition in sloths. *Zoological Journal of the Linnean Society* **178:** 679–712.

Pujos F, Gaudin TJ, De Iuliis G, Cartelle C. 2012. Recent advances on variability, morpho-functional adaptations, dental terminology, and evolution of sloths. *Journal of Mammalian Evolution* **19:** 159–169.

R Development Core Team. 2013. *R: a language and environment for statistical computing*. Vienna: R Foundation for Statistical Computing. Available at: http://www.r-project.org/

Reguero MA, Candela AM, Alonso RN. 2007. Biochronology and biostratigraphy of the Uquía Formation (Pliocene–early Pleistocene, NW Argentina) and its significance in the Great American Biotic Interchange. *Journal of South American Earth Sciences* **23:** 1–16.

Renne PR, Mundil R, Balco G, Min K, Ludwig KR. 2010. Joint determination of ^{40}K decay constants and $^{40}Ar^*/^{40}K$ for the Fish Canyon sanidine standard, and improved accuracy for $^{40}Ar/^{39}Ar$ geochronology. *Geochimica et Cosmochimica Acta* **74:** 5349–5367.

Rincón AD, Solórzano A, McDonald HG, Flores MN. 2016. *Baraguatherium takumara*, gen. et sp. nov., the earliest mylodontoid sloth (Early Miocene) from northern South America. *Journal of Mammalian Evolution* **24:** 179–191.

Rinderknecht A, Bostelmann E, Perea D, Lecuona G. 2010. A new genus and species of Mylodontidae (Mammalia: Xenarthra) from the late Miocene of southern Uruguay, with comments on the systematics of the Mylodontinae. *Journal of Vertebrate Paleontology* **30:** 899–910.

Robertson JS. 1976. Latest Pliocene mammals from Haile XV A, Alachua County, Florida. *Bulletin of the Florida Museum of Natural History* **20:** 111–186.

Rovereto C. 1914. Los estratos araucanos y sus fósiles. *Anales del Museo Nacional de Buenos Aires* **25:** 1–249.

Saint-André P-A. 1994. *Contribution à l'étude des grands mammifères du Néogène de l'altiplano bolivien*. Unpublished D. Phil. Thesis, Museum national d'Histoire naturelle de Paris.

Saint-André P-A, Pujos F, Cartelle C, De Iuliis G, Gaudin TJ, McDonald HG, Mamani Quispe B. 2010. Nouveaux paresseux terrestres (Mammalia, Xenarthra, Mylodontidae) du Néogène de l'Altiplano bolivien. *Geodiversitas* **32:** 255–306.

Scillato-Yané GJ. 1976. El más antiguo Mylodontinae (Edentata, tardigrada) conocido: *Glossotheriopsis pascuali* n. gen., n. sp., del "Colloncurense" (Mioceno Superior) de la provincia de Río Negro (Argentina). *Ameghiniana* **13:** 333–334.

Scillato-Yané GJ. 1977. Octomylodontinae: nueva subfamilia de Mylodontidae (Edentata, Tardigrada). Descripción del cráneo y mandíbula de *Octomylodon robertoscagliai* n. sp., procedentes de la formación Arroyo Chasico (edad Chasiquense, Plioceno temprano) del sur de la provincia de Buenos Aires (Argentina). Algunas consideraciones filogenéticas y sistemáticas sobre los Mylodontoidea. *Publicaciones del Museo Municipal de Ciencias Naturales de Mar del Plata «Lorenzo Scaglia»* **2:** 123–140.

Shockey BJ, Anaya F. 2008. Postcranial osteology of mammals from Salla, Bolivia (late Oligocene): form, function, and phylogenetic implications. In: Sargis EJ, Dagosto M, eds. *Mammalian evolutionary morphology: a tribute to Frederick S. Szalay*. Dordrecht: Springer, 135–157.

Shockey BJ, Anaya F. 2011. Grazing in a new late Oligocene mylodontid sloth and a mylodontid radiation as a component of the Eocene-Oligocene faunal turnover and the early spread of grasslands/savannas in South America. *Journal of Mammalian Evolution* **18:** 101–115.

Shockey BJ, Croft DA, Anaya F. 2007. Analysis of function in the absence of extant functional homologues: a case study using mesotheriid notoungulates (Mammalia). *Paleobiology* **33:** 227–247.

Slater GJ, Cui P, Forasiepi AM, Lenz D, Tsangaras K, Voirin B, de Moraes-Barros N, MacPhee RD, Greenwood AD. 2016. Evolutionary relationships among

extinct and extant sloths: the evidence of mitogenomes and retroviruses. *Genome Biology and Evolution* **8:** 607–621.

Steinmann G. 1929. *Geologie von Peru*. Heidelberg.

Stock C. 1925. Cenozoic gravigrade Edentates of Western North America with special reference to the Pleistocene Megalonychinae, and Mylodontidae of Rancho La Brea. *Carnegie Institution of Washington Publications* **331:** 1–206.

Suárez-Soruco R, Díaz-Martínez E. 1996. Léxico estratigráfico de Bolivia. *Revista Técnica de Yacimientos Petroliferos Fiscales Bolivianos* **17:** 1–227.

Takai F. 1982. Fossil mammals from the Tarija basin, Bolivia. *The Research Institute of Evolutionary Biology* **3:** 1–72.

Takai F, Arózqueta B, Mizuno T, Yoshida A, Kondo H. 1984. On fossil mammals from the Tarija Department, Southern Bolivia. *Contribution from the Research Institute of Evolutionary Biology* **4:** 1–63.

Toledo N. 2016. Paleobiological integration of santacrucian sloths (Early Miocene of Patagonia). *Ameghiniana* **53:** 100–141.

Tomassini RL, Montalvo CI, Deschamps CM, Manera T. 2013. Biostratigraphy and biochronology of the Monte Hermoso Formation (early Pliocene) at its type locality, Buenos Aires Province, Argentina. *Journal of South American Earth Sciences* **48:** 31–42.

Webb SD. 1989. Osteology and relationships of *Thinobadistes segnis*, the first mylodont sloth in North America. In: Redford KH, Eisenberg JF, eds. *Advances in neotropical mammalogy*. Gainesville: Sandhill Crane Press, 469–532.

SUPPORTING INFORMATION

Additional Supporting Information may be found in the online version of this article at the publisher's web-site:

Appendix S1. Referred material.
Appendix S2. 'Toba 76' dating methodology.
Appendix S3. Detailed results of the 'Toba 76' dating.
Appendix S4. Explanation and depiction of the craniodental measurements.
Appendix S5. Craniodental measurements of *Simomylodon uccasamamensis*.
Appendix S6. Additional information for principal components analyses (eigenvalues and loadings).
Appendix S7. Additional information for phylogenetic analysis (codification and support values).
Appendix S8. Chronological and geographical distribution of the taxa.
Appendix S9. Best current estimates of SALMAs and NALMAs (modified from Slater *et al.*, 2016).